A PERFORMANCE INVESTIGATION OF A MULTI STAGED HYDROKINETIC TURBINE FOR RIVER FLOW

KERISHMAA THEAVY A/P KUNALAN

BACHELOR OF ENGINEERING (HONS) CIVIL
UNIVERSITI TEKNOLOGI PETRONAS

JANUARY 2021

A Performance Investigation of a Multi Staged Hydrokinetic Turbine for River Flow

by

Kerishmaa Theavy A/P Kunalan

24488

Dissertation submitted in partial fulfilment of

the requirements for the

Bachelor of Engineering (Hons)

(Civil Engineering)

JANUARY 2021

Universiti Teknologi PETRONAS,

32610, Bandar Seri Iskandar,

Perak Darul Ridzuan

CERTIFICATION OF APPROVAL

A Performance Investigation of a Multi Staged Hydrokinetic Turbine for River Flow

by

Kerishmaa Theavy A/P Kunalan
24488

Dissertation submitted to the
Civil Engineering Programme
Universiti Teknologi PETRONAS
in partial fulfilment of the requirement for the
BACHELOR OF ENGINEERING (Hons)
(CIVIL ENGINEERING)

Approved by,

_____

(Dr Ng Cheng Yee)

UNIVERSITI TEKNOLOGI PETRONAS
BANDAR SERI ISKANDAR, PERAK
January 2021

CERTIFICATION OF ORIGINALITY

This is to certify that I am responsible for the work submitted in this project, that the original work is my own except as specified in the references and acknowledgements, and that the original work contained herein have not been undertaken or done by unspecified sources or persons.

Kerishmaa

_____

KERISHMAA THEAVY A/P KUNALAN

ABSTRACT

Our world has been relying on non-renewable energy based on fossil fuels and coal until these energy sources are depleting day by day and giving impact to the environment. To overcome this environmental impact, governments have started to explore renewable energy sources for example solar, biomass, wind and hydro power. Each of this source has their own way to generate electricity. Wind energy is one of the highest power generation resources then hydro takes over as large portion of the world is water. Dam and turbine application had been used to produce electricity using hydro but the power does not support the rural areas because the application is large and need a huge water resource. Savonius Turbine is proposed because it can generate electricity using the low velocity river flow and less construction cost. Most of the research done currently is only based on one stage rotor and researchers found that one rotor design output is low. The aim of this study is to investigate the performance of the single stage and two stages hydrokinetic turbine for river flow. This study will be investigated by numerical simulation that inclusive of modelling, testing, analyzing the data, comparing the data with existing literature results and also identifying the solution. This data will be collected and analyzed thoroughly so the two stages Savonius hydrokinetic turbine can be proposed. Important parameters such as torque, power as well as the drag force were measured at different azimuthal angle and tip speed ratio. The maximum power coefficient for velocity of 0.86m/s to be at 0.322 at the top speed ratio of 0.767. This is 8.1% improvement in efficiency power coefficient when compared to single stage. The use of two stages will enable power to be extracted more efficiently from low velocity water flow.

ACKNOWLEDGEMENTS

First and foremost, I would like to express my deepest gratitude to Dr Ng Cheng Yee, my Final Year Project supervisor for her continuous guidance and advises on this project. She has greatly contributed to the completion of this project through her great ideas and continuous encouragement for the 8 months. Despite unavailable of having face to face meetings, she always has weekly online meeting to know our progress.

Secondly, my thanks are extended to Mr Mauldar Nauman Riyaz, General and Research Assistant of Dr Ng Cheng Yee for being a great mentor since the starting of my Final Year Project course. He has assisted me throughout the project especially in the software modelling and dissertation. His constant guidance has helped me achieve the objectives of my project.

Finally, my sincere appreciation also extended to my parents and family for their support and patience. I also thank my course mates and friends who have provided assistance and support through various ways. Thank you so much.

TABLE OF CONTENT

LIST OF FIGURES

List of Tables

List of Symbols

Cp:	Coefficient of Power
Ct:	Coefficient of Torque
λ:	Tip Speed Ratio
U:	Speed of water
ω:	Angular velocity
ρ:	Water density
Rε:	Reynolds Number

List of Abbreviations

HKT:	Hydrokinetic Turbine
HAHT:	Horizontal Axis Hydrokinetic Turbine
VAHT:	Vertical Axis Hydrokinetic Turbine
SHT:	Savonius Hydrokinetic Turbine
TSR:	Tip Speed Ratio
AR:	Aspect Ratio
3D:	3 Dimensional

CHAPTER 1
INTRODUCTION

In this part, the background of the overall project, as well as the problem statement, objectives and scope of study will be written.

1.1 **Background of Study**

There is an increase in world energy consumption. Our continued dependency on the non-renewable energy or fossil fuels only makes the situation worse. Several studies have estimated that some of the energy sources would be depleted within a century or in few decades time, if we continue consuming the sources at the current pace. Moreover, environmental problems are emanating from the release of the pollutants are causing concern. As a result, it is essential to identify other sources that are sustainable but must also be environmental friendly (Omar bin Yaakob, 2013).

Renewable energy is the energy that naturally replenished. As mentioned in (*International Energy Outlook* October 14, 2020), renewable energy is currently the fastest growing energy source among the other energy sources, which means the energy usage will increase till 2040. Renewable energy such as solar, wind, ocean, hydroelectric and others had been used to replace the consumption of fossil fuels and also the other non-renewable energy. As it is environmentally friendly and very sustainable, the use of renewable energy sources is increasing and the power generation from renewable energy is often sufficient. Nevertheless, they often produce at different times with respect to demand, especially at the local level. One of the big challenges is to develop energy storage solution to meet the local supply-demand imbalances (Liu, Tait, Schellart, Mayfield, & Boxall, 2020). The hydroelectric has a tremendous potential to be one of the developed renewable energy as in 2015, 16.6% of the world's electricity and 70% of all renewable energy was generated from hydropower(Council, 2016).

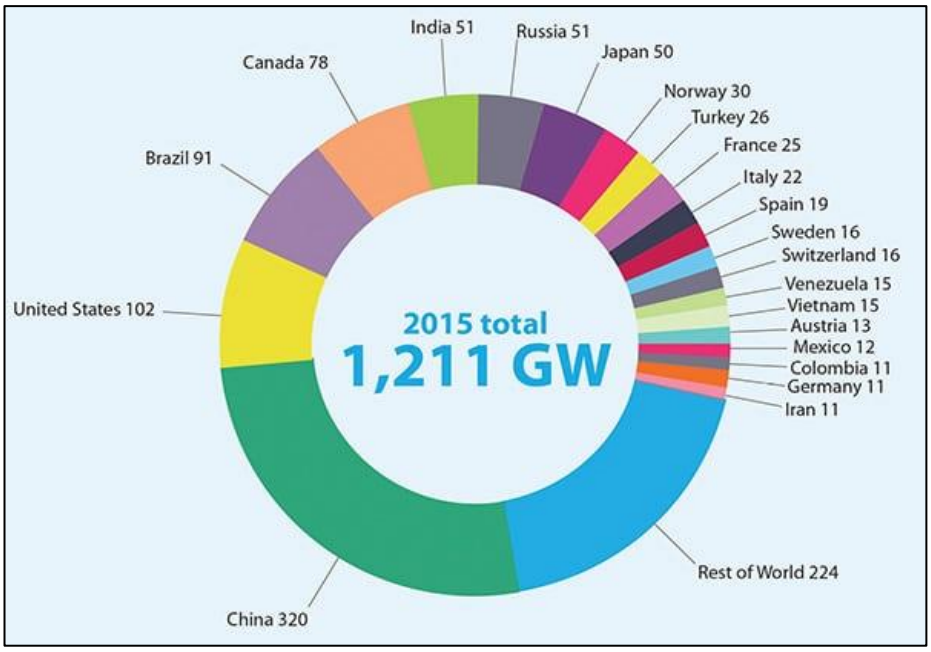

Figure 1.1: Total hydro power installed by end of 2015(Association, May 3, 2016)

Hydroelectric energy is the water that has been stored at the dams. The dam is really useful as it generated electricity roughly 32 percent of global hydro power in 2010 by the Asia Pacific countries (Wikipedia, 15 November 2020). Although this energy is helpful, it effects the topography of the area, communities living place and the marine life in the lake. To avoid this problem, usage of kinetic energy in river flow can be converted into electricity using the current developed technology that is hydrokinetic turbine. Technologies that are able to directly capture the kinetic energy from tidal driven marine current have been developed over the last few decades. Tidal current turbines were preferred over tidal barges because of the flexible system, cost of system and could exceed the requirements of small coastal villages or off-grid areas (Zhou, Benbouzid, Charpentier, Scuiller, & Tang, 2017).

Hydrokinetic Turbine had always known as a technology that been converting kinetic energy into electrical energy. HKT is using the same application as the wind turbine but then this turbine is widely used in the ocean or river flow. From the research paper by Behrouzi, Nakisa, Maimun, and Ahmed (2016), HKT rely on hydrodynamic forces that generate electricity by the fluid flow over the hydrofoil-shaped blades. The turbine can be categorized in horizontal or vertical axis. The horizontal axis design had been preferred by the developers but the vertical axis turbine is still undergoing research and development.

1.2 Problem statement

Consumption of fossil fuels had increased day by day and causes climate change and global warming. Global warming is caused by the increase of the carbon dioxide, methane gas and other greenhouse gases emitted in the atmosphere. The gases are produced from human action such as burning of the fossil fuels, gases coming out from the vehicles and cutting down trees. Besides that, climate change is also the causes of global warming. Intense drought, heat waves, rising of sea levels and warming of oceans had causes the extinction of animals by destroying their places and also it effects the people's livelihoods and communities. Those issues had garnered huge attention and there is a need to explore the alternative sources to replace the non-renewable energy.

Renewable energy are the sources that cannot be replenished and are naturally existed in the world. Solar energy, geothermal energy, biomass, hydro power are the types of renewable energy. Hydropower is one of the potential sources as 70% of the world is water which includes the river water. The main role of hydro power is generating electricity using 2 application. There are dam and hydro kinetic turbine. Both application converts the kinetic energy in the flow and converts into mechanical energy, after that it can generate electricity. The difference between these 2 applications are the size and the volume that can be generated electricity. Dam is applied in the large water flow such as ocean while hydro kinetic turbine is only applied in large and medium water flow e. River flow is not explored as the water level and velocity is low. Besides that, dam and hydro kinetic turbine scale is large and cannot construct in the area. Therefore, the off-grid area not able to receive application.

To overcome this, small scaled turbine such as Savonius Vertical Axis Turbine is introduced but the efficiency is not enough to generate electricity covering the whole area although the velocity is small. To improve the efficiency of Savonius Turbine, few factors are taken into the studies such as the number of rotors, end plate, and many more. Henceforth it is necessary to determine the best set of solutions such as number of rotors end plates to achieve the targeted efficiency within the cost range.

1.3 Objectives

1. To investigate the effect of structural optimization of the existing hydrokinetic turbine design respect to its structural components.

2. To analyze and compare the results of existing and optimized hydrokinetic turbine model.

1.4 Scope of Study

The scope of study in this paper as below:

i. The study is to indicate the Savonius Hydrokinetic Turbine

ii. Incoming velocity value: range within 0.5m/s - 2.5 m/s

iii. Conducting numerical investigation

iv. Software used:
-ANSYS Modelar
-Flow3D

CHAPTER 2

LITERATURE REVIEW

2.1 Renewable Energy

Renewable Energy is the natural resources that are constantly replenished and it is supplied on human timescales (Wikipedia). This energy often consumed in few areas such as power generation, transportation and also heating. The main advantages of this energy sources can reduce the carbon footprint as the renewable energy sources does not discharge harmful pollutants or carbon dioxide into the air like fossil fuels, and coal that releases carbon dioxide when the fossil fuels are heated. The greenhouse effect is caused by carbon dioxide, a gas that traps heat in the Earth's atmosphere. This the process that causes global warming and climates changes. Therefore, renewable energy is a sustainable energy that can help to replace those harmful energy sources. Renewable energy sources are more preferred because it is less expensive as the sources already exist in the world such as the sunlight. Besides that, it gives better health for the community since the reduction of fossil fuels consumption improves the global warming and the climate change scenario. Lastly it improves the world's economy. When generating the energy that produces no greenhouses gas emissions from fossil fuels and reduce the air pollution. According to analysis by Agency (April 2020), global emissions rose 1.7% in 2018 to a record high of more than 33billion tones as energy demand grew by 2.3%.

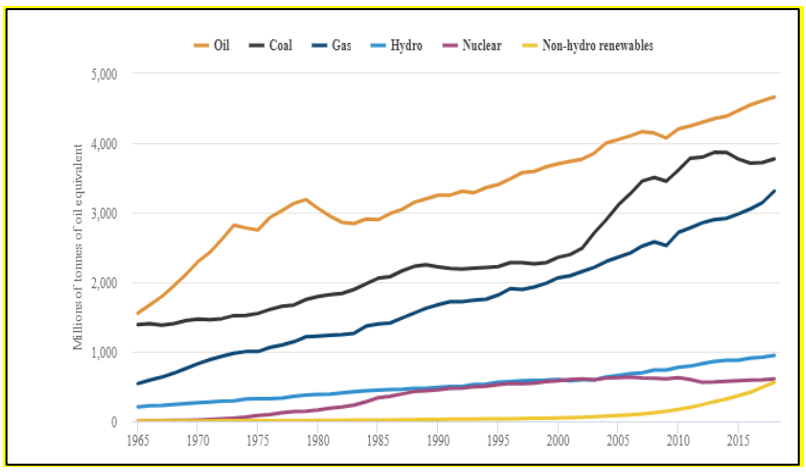

Figure 2.1: Millions of tons of Oil demand from 1965 to 2018 (BP, 1996-2020)

2.2 Types of Renewable Energy

The limited natural resources and the environmental impact of their use require a clean and pollution-free transition soon to renewable energy sources. Among the renewable energy sources such as solar, wind, biomass, hydro and geothermal, mankind has used wind power for centuries because it is plentiful and inexpensive (Alom & Saha, 2019). According to the BP (1996-2020), renewable energy consumption continued to expand rapidly, contributing the highest increase in energy terms (3.2 EJ) ever recorded. Last year, this fuel accounted for more than 40% of global primary energy rise, far more than any other.

2.2.1 Solar Energy

Sunlight is one of the most abundant and freely available energy assets available for our planet. The amount of sunlight that reaches the surface of the earth in an hour is more than the total energy requirements of the planet for a whole year. While it seems like a perfect source of renewable energy, the amount of solar energy that we can use is varied depending on the time of the day, the season of the year and the location. In the UK, solar energy is an increasingly popular way to supplement their energy usage (Wise, 2020).

2.2.2 Wind Energy

The wind is an abundant source of clean energy. With wind energy making an increasing contribution to the National Grid, wind farms are an increasingly familiar sight in United Kingdom (Jones, Pejchar, & Kiesecker, 2015). To collect and transport electricity produced by wind energy, like oil and gas, needs a network of highways, transmission lines, and related infrastructure. While there is domestic or off-grid generation systems, not every land is suitable for a residential wind turbine. By BP (1996-2020) wind generation contributed the most to growth of any energy source(1.4 EJ) , led by solar(1.2 EJ)

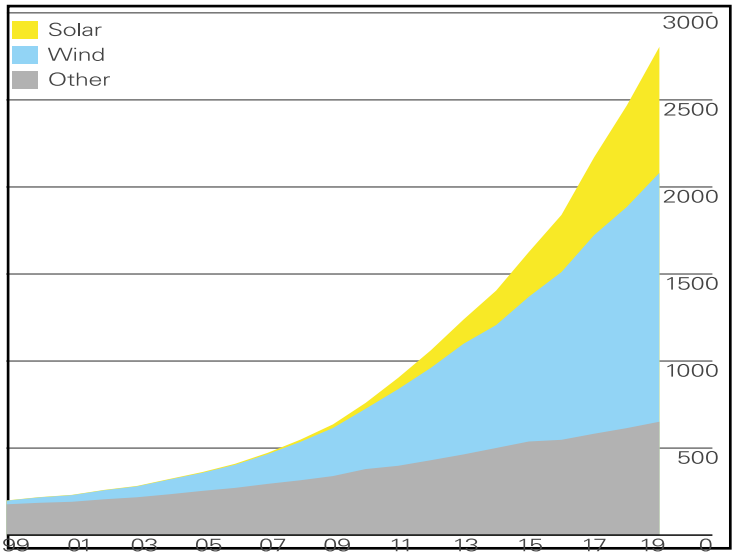

Figure 2.2: Renewable generation by source (terawatt-hours)("Renewable energy consumption, World,")

2.2.3 Biomass

The method of converting solid fuel made of plan materials into electricity is known pyrolysis. Even though biomass is essentially the combustion of organic materials to produce electricity, wood is not burnt, making it a much cleaner and more energy efficient process nowadays. Biomass transforms agricultural, manufacturing, and household waste into solid, liquid, and gas fuel at a lower cost to both the economy and the environment (Headquarters, 1996 - 2020) .

2.3 Hydropower

Of all the renewable energy sources above, hydropower is one of the cleanest and reliable sources. According to the BP (1996-2020) on the power generation from the primary energy, coal is the main fuel for power generation then followed by the renewable energy. In the chart below we can see that hydropower generates 15.6% and highest among the other sources. As mentioned by Evans, Strezov, and Evans (2009) the highest availability, reliability and flexibility of any technology is available for hydropower. In only minutes, hydro plants can be started, stopped, or output rates changed. For this motive, hydro power can provide both base and peak

load power where water resources are adequately plentiful. Hydropower plants have two concepts that can be classified into conventional and unconventional systems.

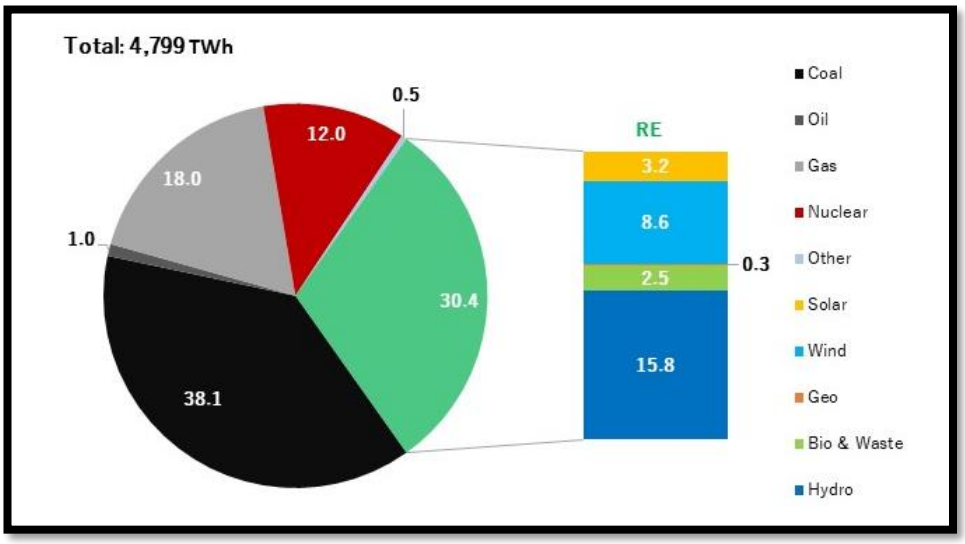

Figure 2.3: World electricity generation mix 2020 (%)(Agency, 25 June 2020)

The conventional system is converted into electrical energy from gravitational energy. This system requires a dam or reservoir that is located in a high place to generate electricity, such as hills. However, as it is a large building, there are some major disadvantages to this system. Dams harm the environment and disrupt the mobility of fish. They can also not be used to extract energy from huge potential sources such as ocean currents or low-grade rivers for power systems (Alexander N. Gorban', December 2001). Therefore, the conventional system is not preferable because it requires a huge site to develop velocity with the maximum head velocity. The unconventional hydropower system is where, without the need for large volumes of water, the kinetic energy from free-flowing water is converted into electric energy. This system is called a hydro kinetic turbine.

2.4 Hydrokinetic Turbine

The turbine rotates when water flows through the turbine and the generator connected to the turbine generates energy. The kinetic energy of moving water is then converted into energy in the process (Tian, Zhang, Yuan, Che, & Zafetti, 2020). Apart from the flowing medium, the hydro kinetic turbine shares similar principles to that of a wind turbine. Because water is about 800 times denser than air, a hydrokinetic turbine will generate more power(C. Boccaletti). Some companies have

also explored the outcomes of hydrokinetic turbines testing (Basumatary, Biswas, & Misra, 2018).

A performance curve is used to rate turbines, and it shows the power coefficient (C_p) as a function of tip speed ratio (λ). It is known the factor of 0.539 is the Betz Limits(Tony Burton, 2001).

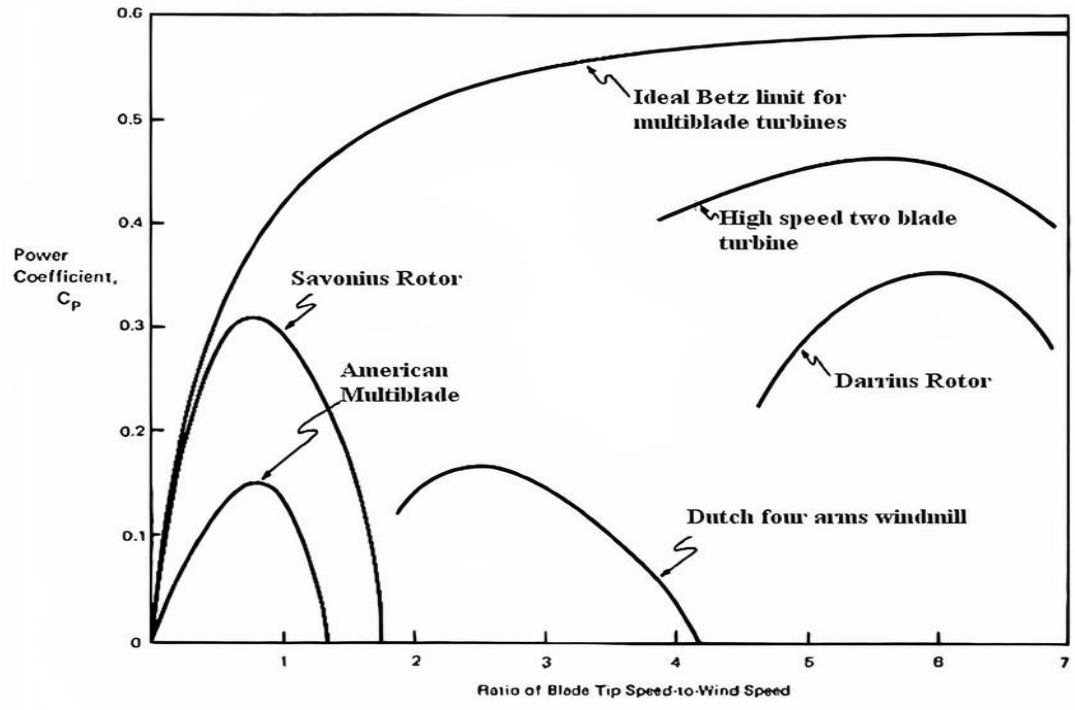

Figure 2.4: Betz limits graph(Ragheb, 2011)

There are two types of Hydrokinetic Turbine and both turbine has 2 different concepts and the way it generates electricity.

2.4.1 Horizontal Axis Hydrokinetic Turbine

Most of this component turbine are installed in Ireland and is function is to extraction the marine current energy (Kailash, Eldho, & Prabhu, 2012).The same ideals as aircraft wings, propellers and wind turbines are used by lift-based, axial-flow turbines. A lift-based turbine's blades are made up of two-dimensional hydrofoil cross-sections. This shaft power is converted into electricity either directly connected to the shaft or through gearbox or indirectly connected via hydraulic transmission by a generator (Laws & Epps, 2016).

2.4.2 Vertical Axis Hydrokinetic Turbine

Vertical axis hydrokinetic turbines (VAHT) rotate around an axis that is perpendicular to the flow direction, widely recognized as the crossflow water turbine. For small-scale power generation, vertical turbines are generally used. This turbine is more cost effective because less maintenance is needed as the electrical component is all above the water surface and easy to construct as the design is very simple(Jing, Sheng, & Zhang, 2014). The vertical-axis HKT systems perform better at lower water flow rates, usually not more than 1.0 m/s, in shallow channels, and with varying water velocities; thus, they are favored in low-power river current applications (Badrul Salleh, Kamaruddin, & Mohamed-Kassim, 2019). H-Darrieus, Darrieus and Savonius are the types of VAHT that is normally used in testing the electricity generation.

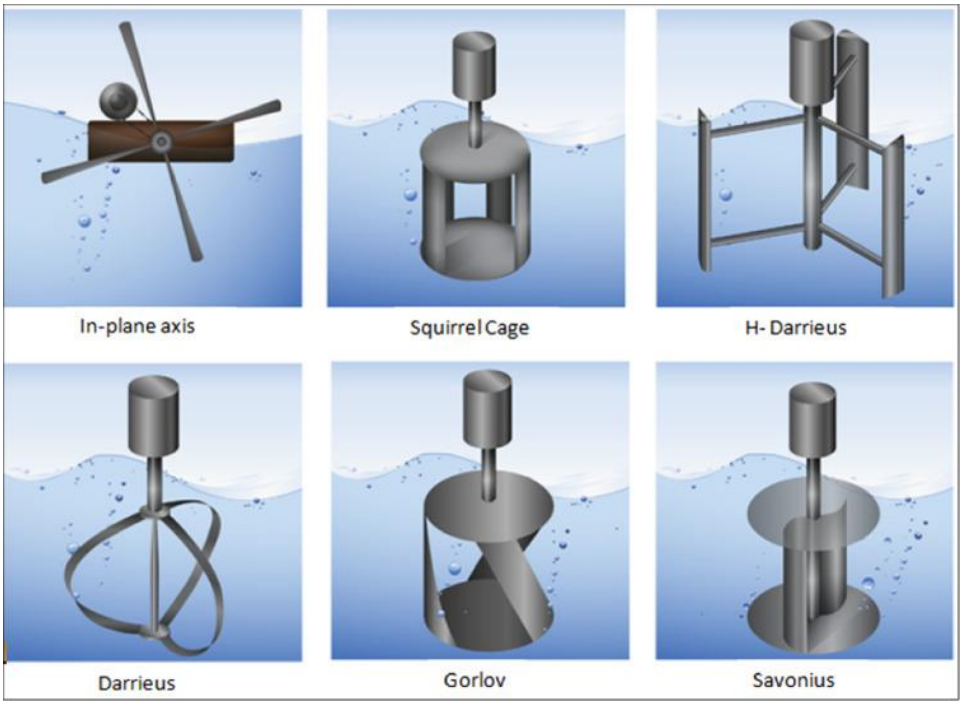

Figure 2.5: Types of vertical hydrokinetic axis turbine

2.5 Savonius Hydrokinetic Turbine

Vertical axis Savonius turbine wind rotor was originally invented by Finish engineer Sigurd J. Savonis in 1920 for wind energy application. It is a drag based energy conversion device and resembles an “S” shape viewed from the top (Parag K. Talukdara, 2008). Compared to plain or convex, concave blades result in a higher value on the drag coefficient, which forces the rotor to rotate when installed in flowing water. Turbine blades are of high strength, which gives a higher starting torque to the turbine than turbines with low-solidity blades with the same force applied from the river. Therefore, the Savonius turbine is self-starting and can provide high torque at relatively low speeds(Ulvmyr, June 2016).

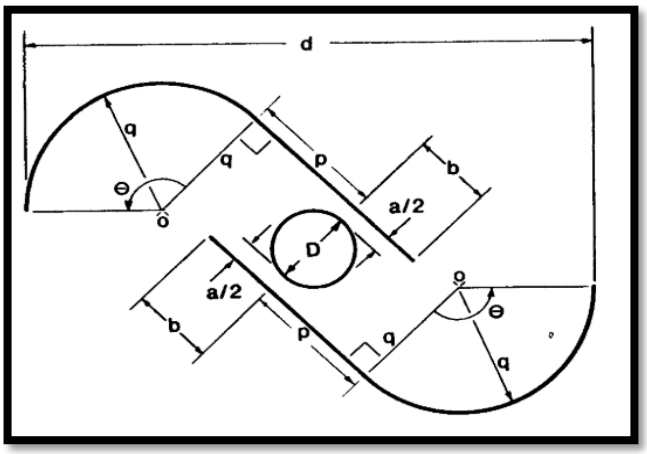

Figure 2.6: Top view of modified Savonius rotor with shaft(Mahalingam Venkatesh, Vijay Babu, & Suresh, 2018)

The turbine has a slightly lower efficiency than the HAHT. Besides that, the turbine size is small so it can be setup at a small area proximity to the river flow. Savonius is useful but it is not well-known like the HAHT due to the poor performance by the turbine.

2.5.1 Performances of Savonius Hydrokinetic Turbine

The tip speed ratio (TSR), λ of the rotor is defined by equation 1 below where U is the speed of water, ω is the angular velocity of the turbine whereas D is the diameter of the modified bach blade.

$$\lambda = \frac{\omega D}{2U}$$

(Eq 1)

$$\omega = \frac{\Delta\theta}{\Delta t}$$

(Eq 2)

The torque coefficient, Ct is the ratio between the torque found in the rotor and the theoretical torque that the water as shown in equation 2. It is given by the torque produced at the advancing and returning blades. T represents the moment of the force, A is the swept area.

$$Ct = \frac{T}{\frac{1}{4}\rho A_s D U^2}$$

(Eq 3)

Power coefficient, Cp is measured as it will affect the overall output of the power estimation. The power coefficient is measured from the function of power, P as shown in equation 3.

$$Cp = \frac{P}{\frac{1}{2}\rho A_s U^3}$$

(Eq 4)

2.6 Techniques of improving the Savonius Hydrokinetic Turbine performance

2.6.1 Effects of number of blades in the turbine

Number of blades in the turbine had always been one of the parameters that can affect the performances. In 2012, Yaakob et al. computationally studied the performance of a two-bladed semicircular SHT and proved that a CPmax of 0.275 at TSR=0.7. In 2014, Sharma et al. tested a three bladed SHT in an open channel at water speed (V)of 0.3–0.9 m/s. The CPmax measured during the experiments was 0.39 at TSR=0.77 which was 61.32% higher than a conventional SHT at similar input values. Other researchers found that the two-blade rotor having higher performance value than three blade rotor. By adding obstacle had improves the self-starting capability of the two blade SHT (Mohamed, Janiga, Pap, & Thévenin, 2010).

2.6.2 Effect of deflector plate position

Deflector plates are placed at the advancing blade size to augment the rotational speed. Golecha et al. performed various experiments on SHT to

enhance the performance of using a deflector plate placed at an optimum position. In such arrangements, they found an increase of the CPmax value by 50%. He varied the deflector plate position on the returning blade side.

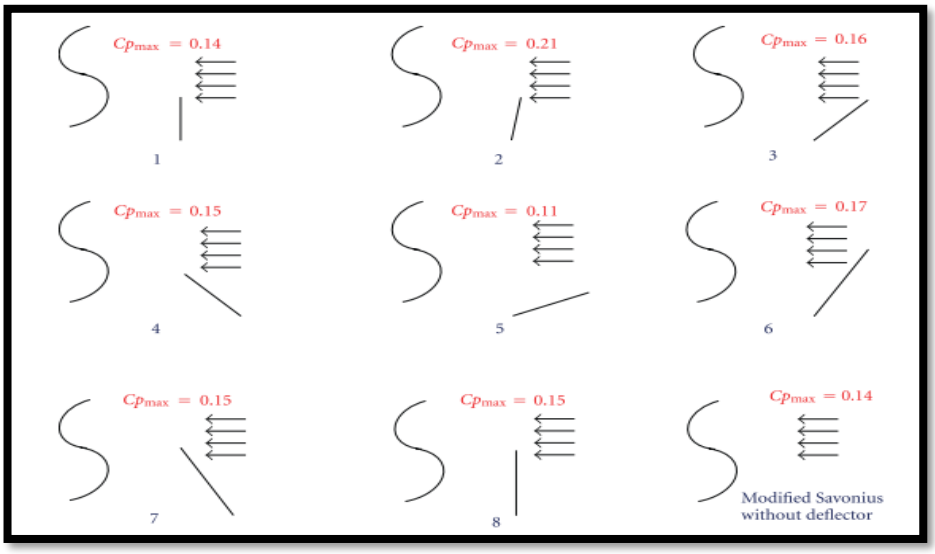

Figure 2.7: Different positioning of deflector plate on the returning blade side(Golecha Kailash, 2012)

2.6.3 Multi-Stage of Savonius hydrokinetic turbine

The experimental study that was carried out by Nakajima et al. reveals that the CP value of SHT was enhanced by 10% with the use of the double stage configuration having 90° phase difference in the blades. Khan et al. found that double stage SHT gives better performances than single and three stage. The CPmax for single, double and three stage semi-circular bladed SHT are 0.038, 0.049 and 0.04 respectively.

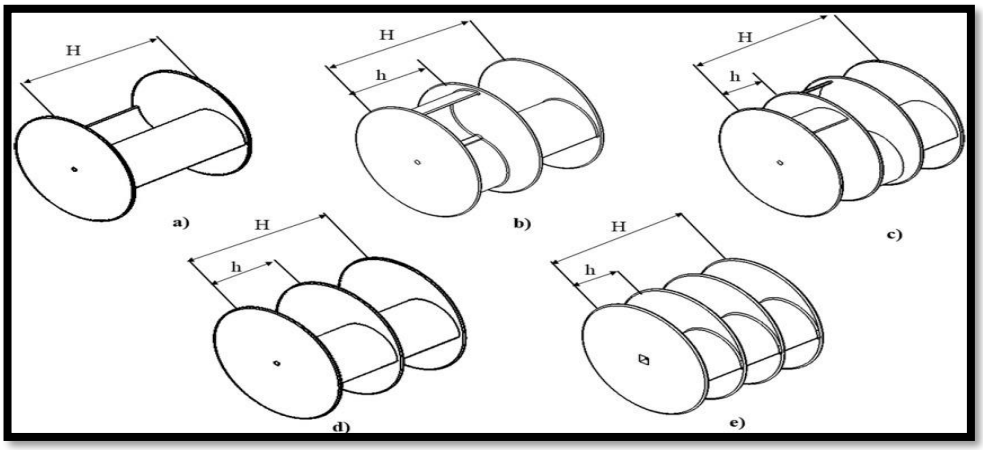

Figure 2.8: Multi-stage Savonius Hydrokinetic Turbine(Mahesa Prabowoputra, Hadi, Sohn, & Prabowo, 2020)

2.6.4 Types of Blade Profile

Semi elliptical is composed from two semi-circular shape. The Benesh profile is composed of a straight line with two arcs. Modified Bach profile composed by a straight line and an arc. Two researchers tested the Benesh profile, modified Bach and the traditional semicircle and the semi elliptical rotor. The Cpmax shown is 0.29,0.30,0.26 and 0.23 respectively (Roy & Saha, 2015).

2.7 Modified Bach Profile

A modified bach blade profile is selected from the recent investigations of Roy and Saha. This blade design is composed by a straight line and an arc. This blade had shown improvements in power coefficient, torque coefficients and aerodynamic characteristics when compared to the conventional SHT. This study is tested on two stage SHT with the modified bach blade design. Table 2.7.1 shows the optimization studies by researchers on SHT for two stages.

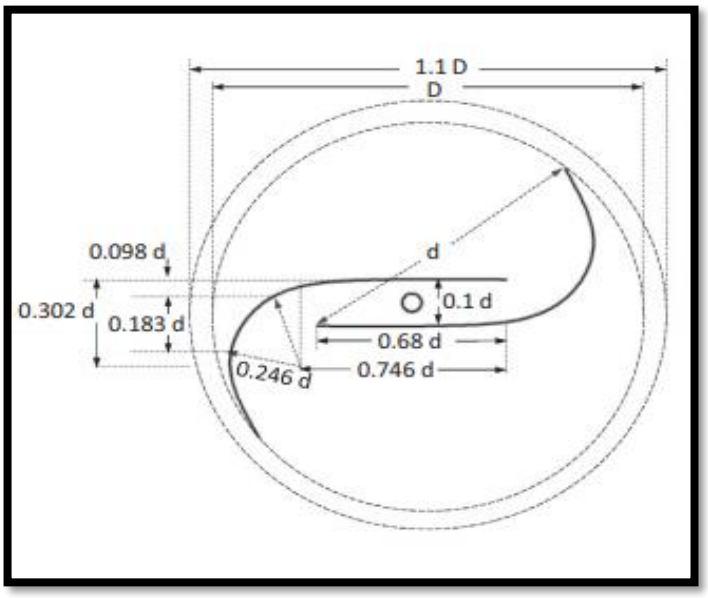

Figure 2.9: Modified Bach Blade Profile(Roy & Saha, 2015)

Table 2.1: Two stage as the optimization of the SHT studies

Types of Energy	**Title**	**Author**	**Findings**
Wind	A double-step Savonius rotor for local production of electricity: a design study	Menet, J. L., 2004	Predicted max delivered power=120W
Wind	Optimum design configuration of Savonius rotor through wind tunnel experiments	Saha,2008	Experimental C_{pmax}=0.21
Water	Performance of Savonius Rotor as a Water Current Turbine	Nahidul Islam Khan, 2009	Experimental C_{pmax}=0.049
Water	Influence of the deflector plate on the performance of modified Savonius water turbine (90 degree phase with deflector plate)	Golecha,2011	Experimental C_{pmax}=0.17 at TSR=0.83
Water	Experimental Studies on Savonius-type Vertical Axis Turbine for Low Marine Current Velocity	Omar Yaakob,2013	Experimental C_{pmax}=0.14
Wind	Performance Measurement of a Two Stage Two Bladed Savonius Rotor	Sharma,2014	Experimental C_{pmax}=0.438 at TSR=0.698
Wind	Numerical and experimental characterization of multi-stage Savonius rotors	Frikha, 2016	Experimental & CFD C_{pmax}=0.081
Wind	Numerical and experimental study of a helical Savonius wind turbine and a comparison with a two-stage Savonius turbine	Kothe,2020	Experimental C_{pmax} =0.128 at TSR=0.655

2.8 Summary of Literature Review

Dams are not appropriate because it is large and costly. It effects the surrounding and living things in the water. It cannot be used to extract energy in the potential area such as low velocity water flow so hydrokinetic turbine is needed. Hydrokinetic turbine can work in medium flow of water as water is 800 times denser than air so it can generate more power. There are 2 types of turbine there are horizontal axis hydrokinetic turbine and vertical hydrokinetic turbine. Savonius utilized as vertical axis hydrokinetic turbine to exploit hydrokinetic energy convert to electricity and it can work well in intermediate to shallow river water. Modified Bach blade has also shown major improvements in power coefficient and torque coefficient. Two stages produce higher power than single, and three stages and the torque have not much variation.

The critical literature review for this study is:

1. Modified bach blade design: increase the power and torque coefficient
2. Two stage SHT: shows better performance than single stage SHT
3. Malaysian ocean current range: the current range is 0.5 to 1.5m/s. In this study we choose the average velocity that is 1m/s.

CHAPTER 3

METHODOLOGY

3.1 Research Methodology

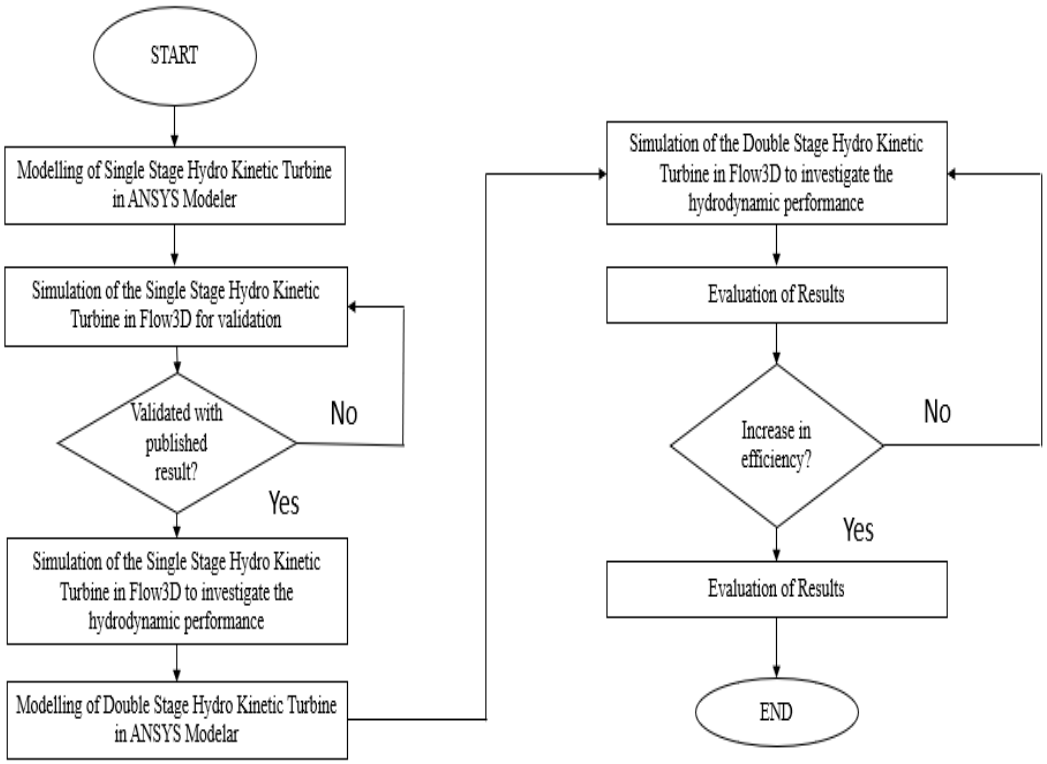

3.2 Modelling

The dimensions are important for estimating the power of the turbine. The geometrical properties design consists of height, AR, rotor diameter. Table 3.1 shows the dimensions of the turbine based on the literature studies. AR is the ratio of height(H) to its diameter(D). A high AR improves the efficiency (Saha,2013). Figure 3.1 and 3.3 shows the single stage and two stages modelling and Figure 3.2 and 3.4 shows the top view of both stages blade design.

Table 3.1: Geometric parameters of the study

Geometric Parameters	**Dimensions**
Diameter of End Plate	191mm
End Plate Thickness	4mm
Height of Single Stage	191mm
Height of Double Stage, H	191mm
Aspect Ratio (H/D)	1
Length of straight segment, L	10mm
Angle of Arc segment	135^0
Shaft Diameter	14mm

Single Stage Hydrokinetic Turbine Model

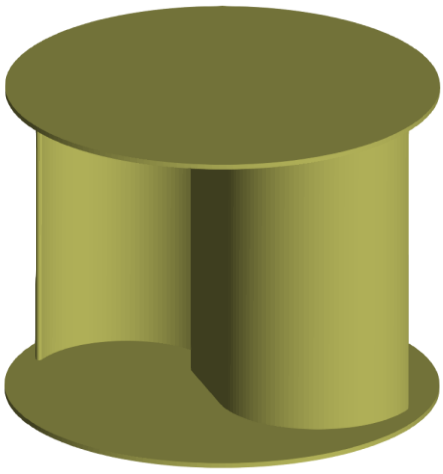

Figure 3.1: Single stage modelling

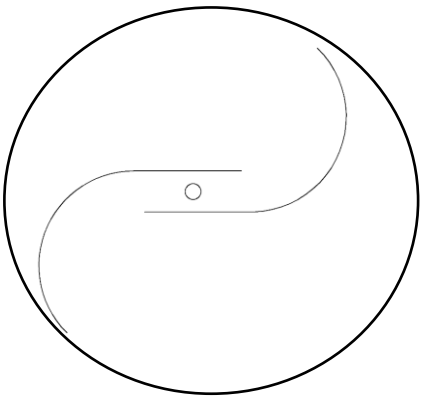

Figure 3.2: Top view of the single Stage blade design

Double Stage Hydrokinetic Turbine Model

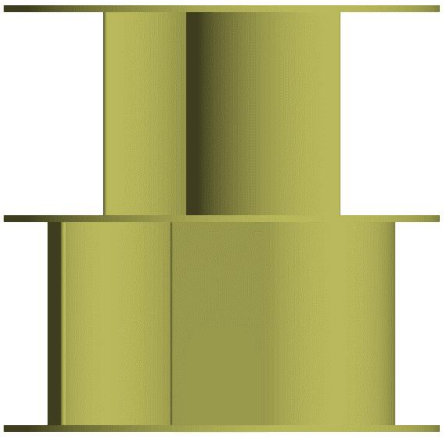

Figure 3.3: Two stage modelling

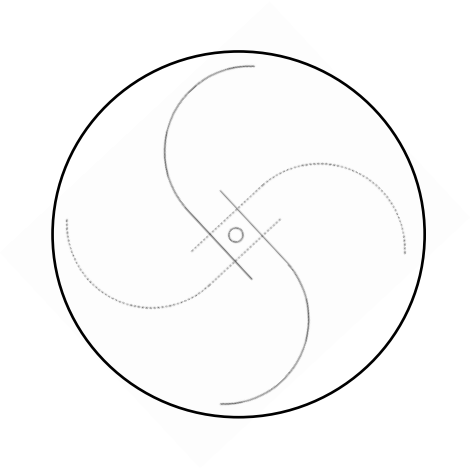

Figure 3.4: Top view of two stage Blade design

3.3 Computational Domain

The standard $k-\varepsilon$ turbulence model is used, which solves 2 separate transport equations and allows the turbulent kinetic energy(k) and its dissipation rate (ε) are to be determined independently. The standard $k-\varepsilon$ turbulence model is superior to other models in that it can be used to solve problems involving fluid flow in the vicinity of complex geological structures. Due to the model using wall functions based on the law of the wall, sharp corners, straight and curved edges, such as those of the turbine blades, it can be easily determined and covered for executing the computing process (Sarma et al., 2014).

Figure 3.5 presents the 3D computational domain with the Savonius rotor created using the Flow3D. The stationary zone is characterized by 2m length, 0.89m width and 1.4m height. The rotating zone is created by using an enclosure with a diameter equal to 1.2 times times the diameter of the Savonius rotor(Mosbahi et al., 2021). Diameter of the blade is 0.174m and diameter for the end plate is 0.191m. Minimum dimension of the upstream turbine in the computational domain is 2 times diameter of the blade. The height is at least 4 times of the diameter of the blade.

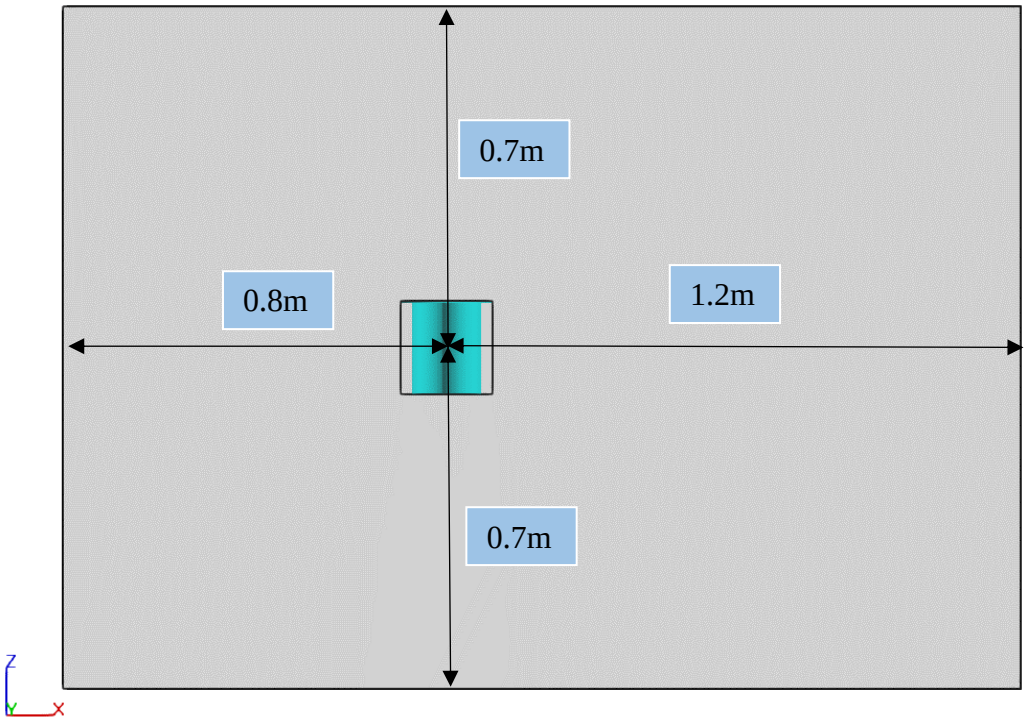

Figure 3.5: Front view of the computational domain

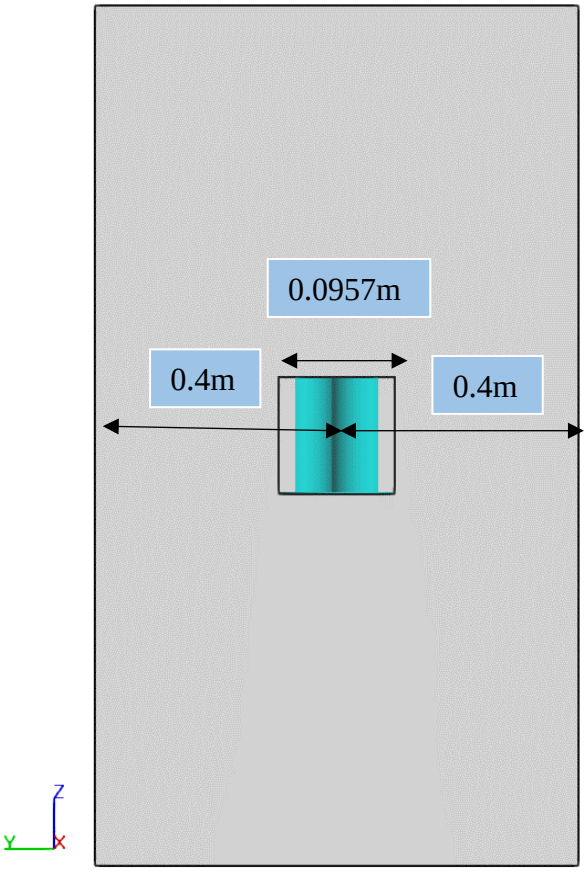

Figure 3.6: Side view of the computational domain

3.4 Boundary Condition

The boundary condition are shown in Figure 3.7, a water velocity of 0.86m/s at the inlet boundary condition so the flow can travel through the domain(Kacprzak & Sobczak, 2014). Once the flow had interacted with the turbine, it flows through the outlet boundary condition. Outlet acts smooth flow outside the computational domain and it only flow in one way. To improve the stability of the numerical simulations, symmetrical boundary condition is applied for the side wall of big domain and the 4 sides of small domain(Tian, Mao, & Ding, 2018). The big domain symmetrical acts as blockage where the flow will not reflect to the turbine and effect the rotation. The small domain boundary is to make it finer and can be read properly by the solver. Besides that, it is assumed that the turbine operates as the proper depth in order to reduce the surface effect and free surface effects are neglected in the simulation.

Table 3.2: Terms of boundary condition

Boundary Condition	
V	Velocity
O	Outlet
S	Symmetrical

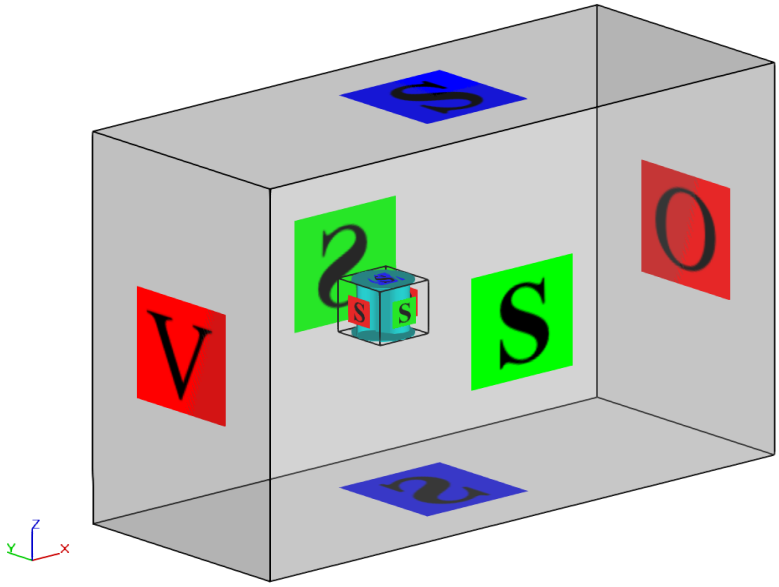

Figure 3.7: Schematic diagram of boundary condition

3.5 CFD Setup

In CFD procedure, Flow3D have been used to generate the results. After completing the meshing process, at the general sub-tab. The working fluid is only one fluid which is water. There is no any sharp interface in this turbine. Different materials can also been assigned in this tab.

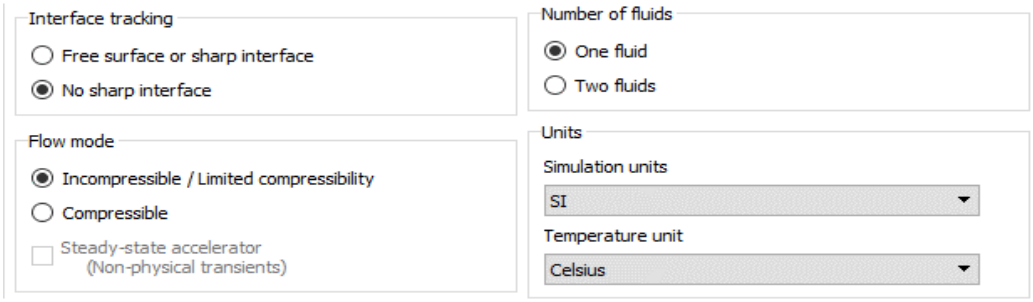

Figure 3.8: Assign number of fluid

In the moving object setup sub-tap as shown in this Figure 3.9. This set involves the rotational axis and its angular velocity in the body system. Since only one body is identified as rotational and another one is considered stationary. The rotational axis for both domains will be in the same axis. This sample has been the set for TSR of 0.767 The angular velocity is set to -11.318 rad/s rotates along the z axis. This value is calculated from the Equation 2. The negative sign is because the Savonius rotor rotates in clockwise.

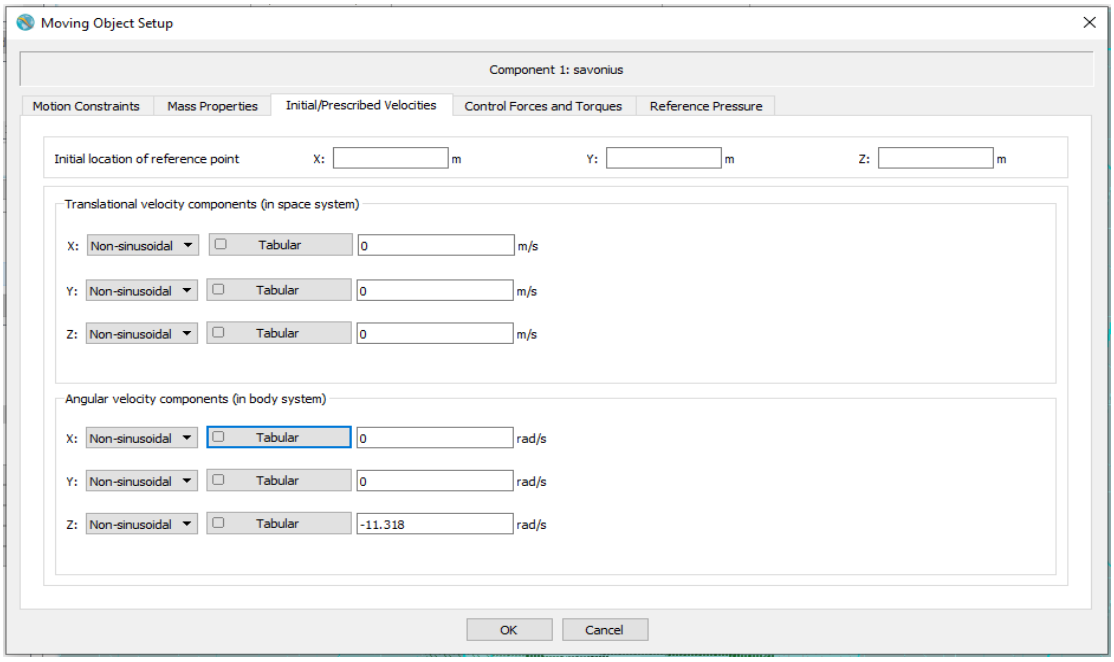

Figure 3.9: Moving object setup

In this set, general moving objects is activated. Then under the moving object slot, implicit is selected. Implicit is when the dependent variables are defined by coupled sets of equation and iterative technique is needed to obtain the solution. The material density 7850kg/m^3 is more than the density of water 1000kg/m3 so implicit is ticked. In figure 3.10 as known only one fluid is used. Second order monotonicity preserving is selected under momentum advection so the mesh domain can capture the flow of water well.

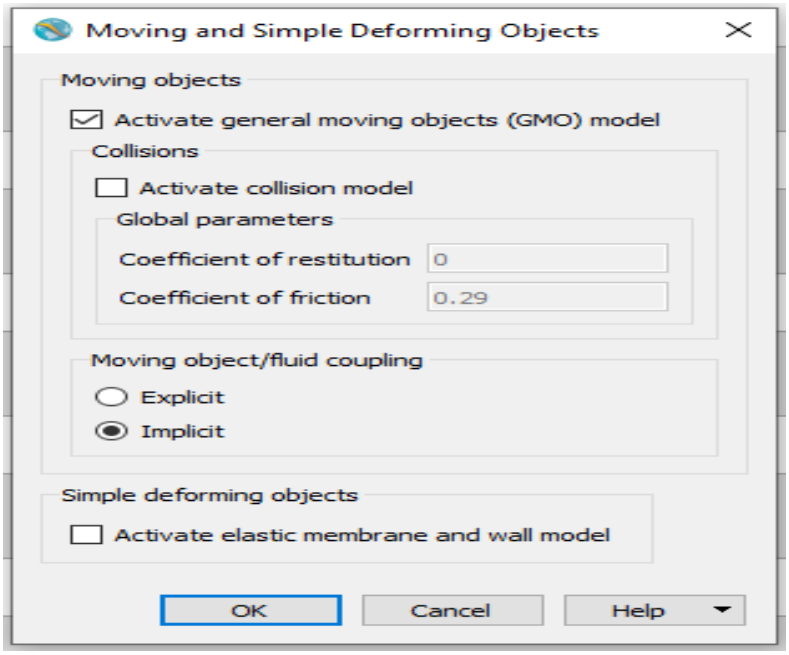

Figure 3.10: Moving and simple deforming objects 1

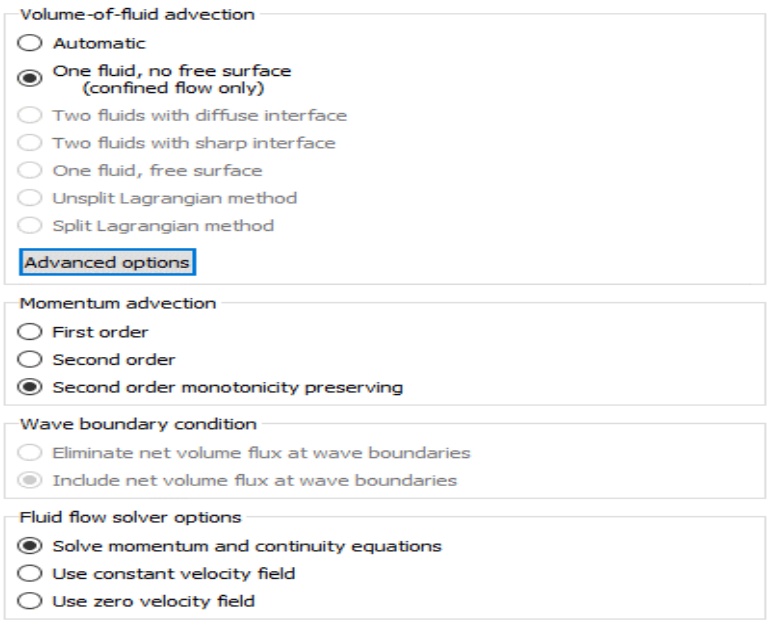

Figure 3.11: Moving and simple deforming object 2

Before starting the simulation, simulation pre-check is done for mesh block 1(big domain) and mesh block 2(small domain). To define a good mesh quality, the maximum aspect ratios for all the axis must be less than 1.2. This shows the mesh satisfy the 3D model.

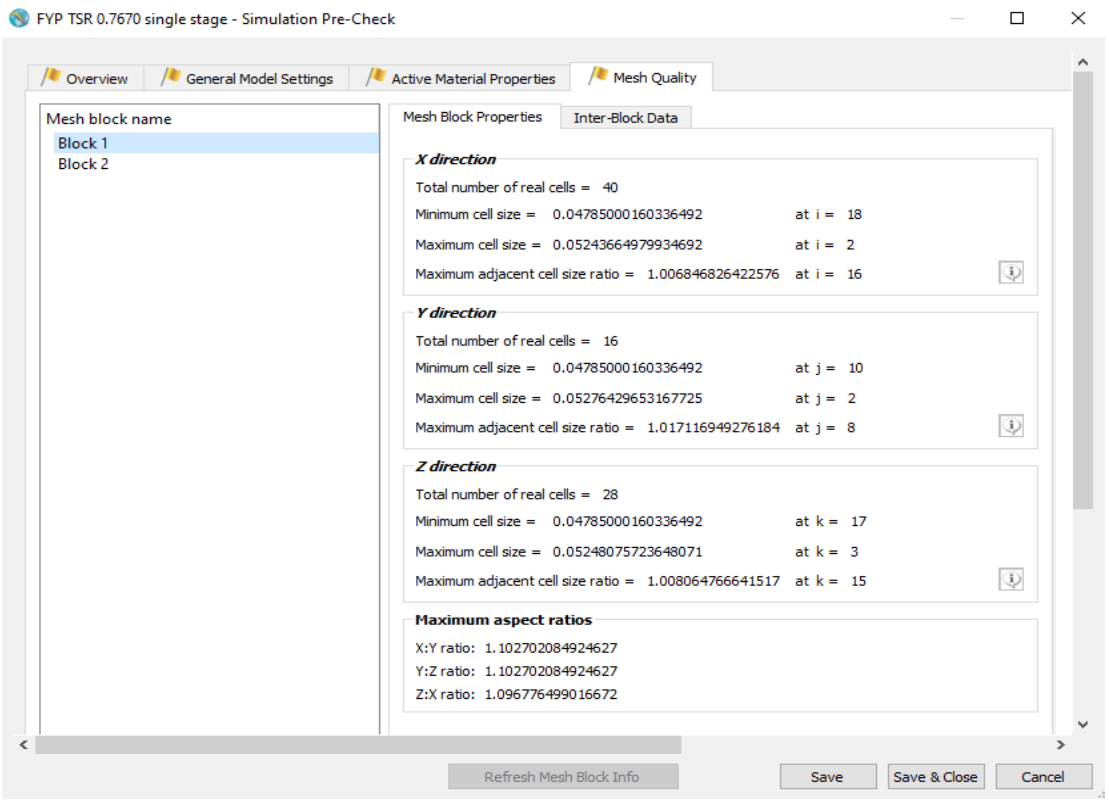

Figure 3.12: Simulation pre-check process for mesh block 1

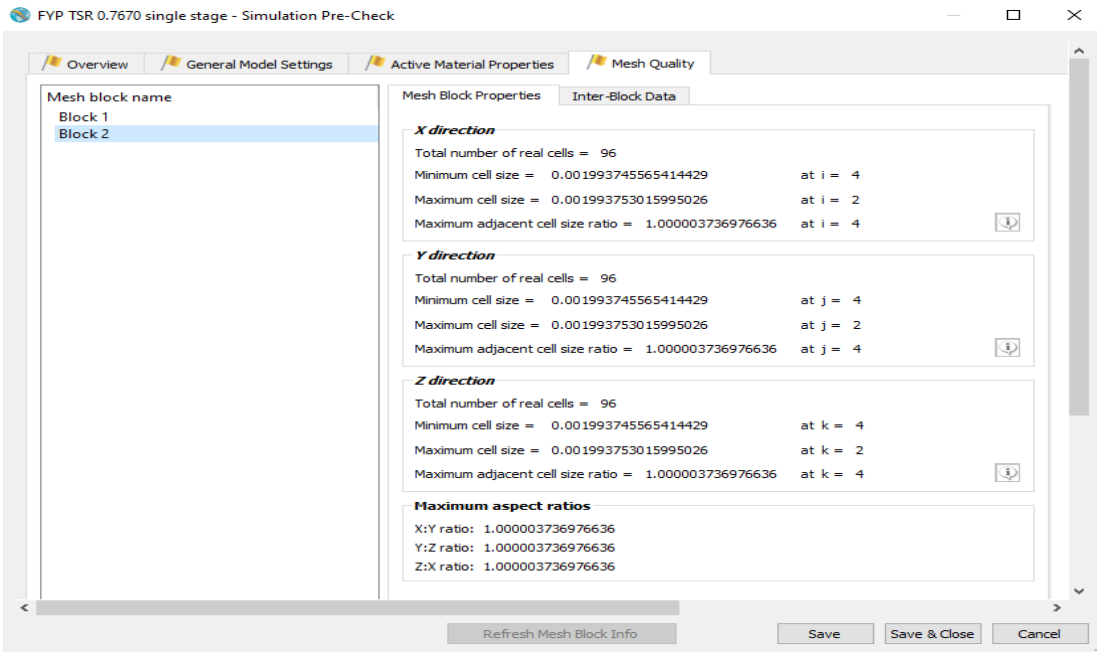

Figure 3.13: Simulation pre-check process for mesh block 2

After the simulation pre-check is satisfied, then start the simulation. The results of the simulation will be as Figure 3.14 The red line is the stability limit while the blue line is time-step size. To get a stable result, the red and blue line must converge together. If the red line is not moving away from the blue line then the limit is stable.

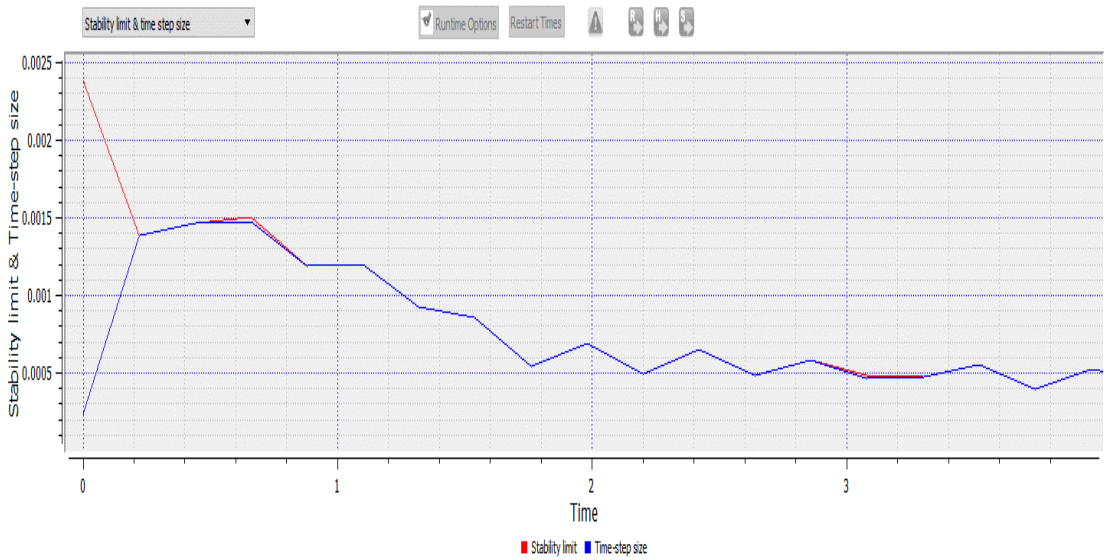

Figure 3.14: Results of the simulation

In Figure 3.15, is the results generated for each time-step. To identify a steady result, in the pressure iteration column, the data generated must be between 0.2 to 1. Concluded the simulation is success for that TSR.

progress		time step		pressure		performance			
sim_time	cycle	delt	dt_stbl/code	iter	res/epsi	el_time	%PE	clk_time	est_rem_time
2.03703E+01	101150	2.01E-04	2.01E-04/cx	1	4.66E-01	1:12:43:23	87	21:21:48	02:56:14
2.04600E+01	101617	2.25E-04	2.25E-04/vs	1	3.74E-01	1:12:53:23	85	21:31:48	02:46:33
2.05542E+01	102079	1.77E-04	1.77E-04/vs	1	5.17E-01	1:13:03:24	87	21:41:49	02:36:22
2.06471E+01	102540	2.20E-04	2.20E-04/vs	1	5.25E-01	1:13:13:24	86	21:51:50	02:26:18
2.07360E+01	103005	2.06E-04	2.06E-04/cx	1	2.82E-01	1:13:23:25	87	22:01:50	02:16:43
2.08305E+01	103469	1.77E-04	1.77E-04/vs	1	2.41E-01	1:13:33:25	86	22:11:51	02:06:29
2.09234E+01	103932	2.19E-04	2.23E-04/vs	1	5.74E-01	1:13:43:27	87	22:21:52	01:56:26
2.10129E+01	104399	2.19E-04	2.19E-04/vs	2	1.35E-01	1:13:53:28	85	22:31:53	01:46:46
2.11075E+01	104863	1.77E-04	1.77E-04/vs	1	2.92E-01	1:14:03:29	85	22:41:54	01:36:32
2.11999E+01	105324	2.05E-04	2.05E-04/cx	1	5.08E-01	1:14:13:30	85	22:51:55	01:26:32
2.12885E+01	105787	2.04E-04	2.04E-04/cx	1	3.72E-01	1:14:23:30	85	23:01:55	01:16:58
2.13838E+01	106252	1.76E-04	1.76E-04/vs	1	4.41E-01	1:14:33:31	85	23:11:56	01:06:39

```
============= mentor tip ===============
      solution is nearly steady:
      variation from the mean is
 less than   3.4446E-02 %  at t=  2.13852E+01
=========================================
```

Figure 3.15: Pressure iteration to identify stable results

3.6 Mesh Density Analysis

The process of simulation is done by repeating with varying refinement levels of the mesh. The refinement is carried on undertaking different mesh sizes. In the table below shows the number of mesh cells and the mesh cell block for big and small is tested to get the acceptable C_t result.

Table 3.3: Mesh density analysis

Refinement level	No. of mesh cells	Mesh cell size	
		Bigger mesh block (mm)	Smaller mesh block(mm)
1	4.08x10^5	18	8
2	6.75x10^5	15	7
3	1.10x10^6	13	5.5
4	1.17x10^6	13	4
5	2.43x10^6	10	3
6	2.62x10^6	10	2.5
7	3.97 x 10^6	9	2

3.7 Validation for Power Coefficient & Torque Coefficient

CFD analysis should go through the process of validation. The results obtained have to be compared to experimental data in the literature in order to assess their accuracy. Below table shows the TSR and the experimental value of C_p and C_t obtained from the literature result(Roy & Saha, 2015).

Table 3.4: TSR vs C_p experimental

TSR	Experimental
0.158	0.091
0.273	0.15
0.365	0.194
0.451	0.23
0.503	0.243
0.566	0.256
0.661	0.275
0.767	0.279
0.859	0.268
0.948	0.247
1.005	0.224
1.091	0.182
1.145	0.144

Table 3.5: TSR vs C_t experimental

TSR	Experimental
0.158	0.576
0.273	0.549
0.365	0.532
0.451	0.510
0.503	0.483
0.566	0.452
0.661	0.416
0.767	0.364
0.859	0.312
0.948	0.261
1.005	0.223
1.091	0.167
1.145	0.126

3.8 Gantt Chart

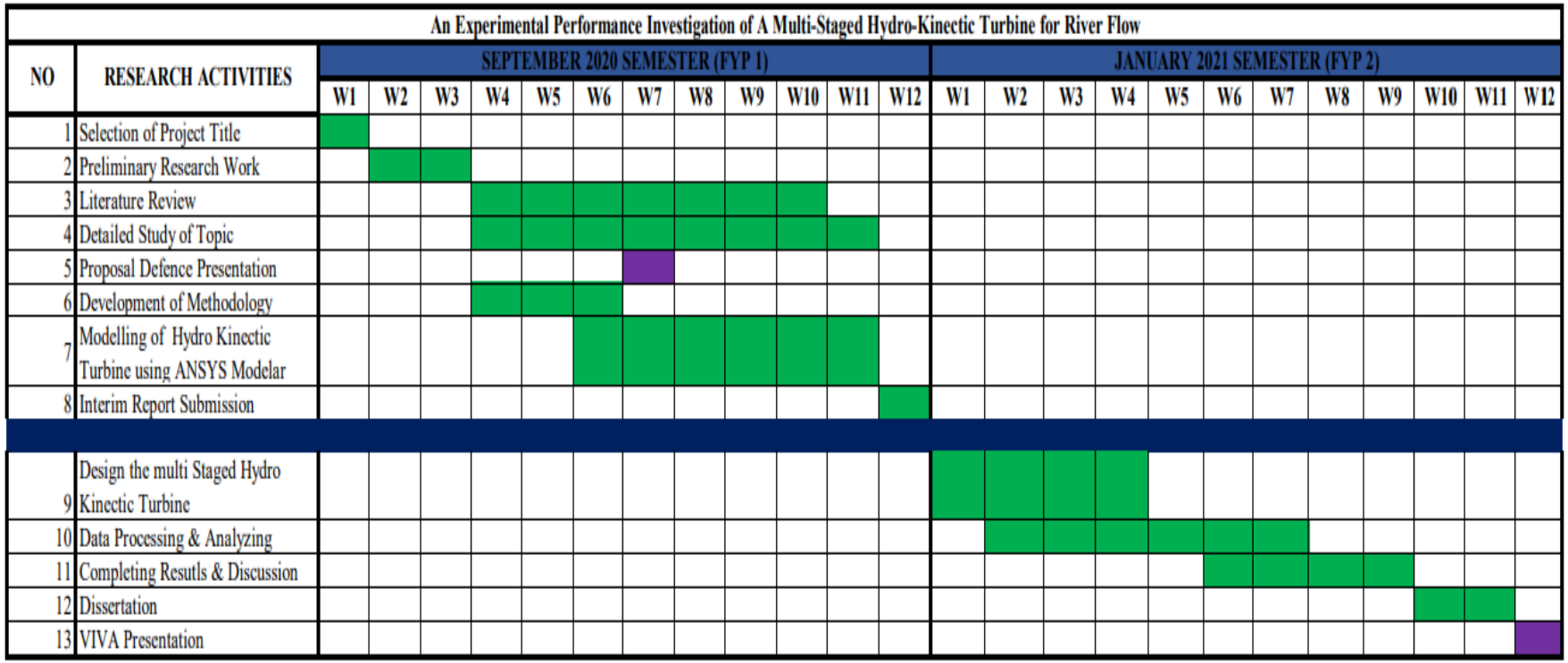

Figure 3.16: FYP gantt chart

CHAPTER 4

RESULTS & DISCUSSION

4.1 Validation for Mesh Density Analysis

Based on section 3.6, mesh density analysis is tested to know the mesh cell size that is suitable for the model. Refinement level 5 was selected because the C_t value is acceptable. A smooth mesh ensures the uniform geometry shape. Bad mesh leads to changes in geometry such as rough and uneven surfaces that affect the simulation results. The biggest mesh block size is 10mm and the smallest mesh block size is 3mm. The difference of the mesh block size can be seen through Figure 4.1. This is spinar mesh where the bigger mesh block collide with the small mesh block.

Table 4.1: Mesh density analysis

Refinement level	**No. of mesh cells**	**Mesh cell size**		C_t
		Bigger mesh block (mm)	**Smaller mesh block(mm)**	
1	4.08x10^5	18	8	0.3
2	6.75x10^5	15	7	0.38
3	1.10x10^6	13	5.5	0.44
4	1.17x10^6	13	4	0.39
5	2.43x10^6	10	3	0.43
6	2.62x10^6	10	2.5	0.43
7	3.97 x 10^6	9	2	0.42

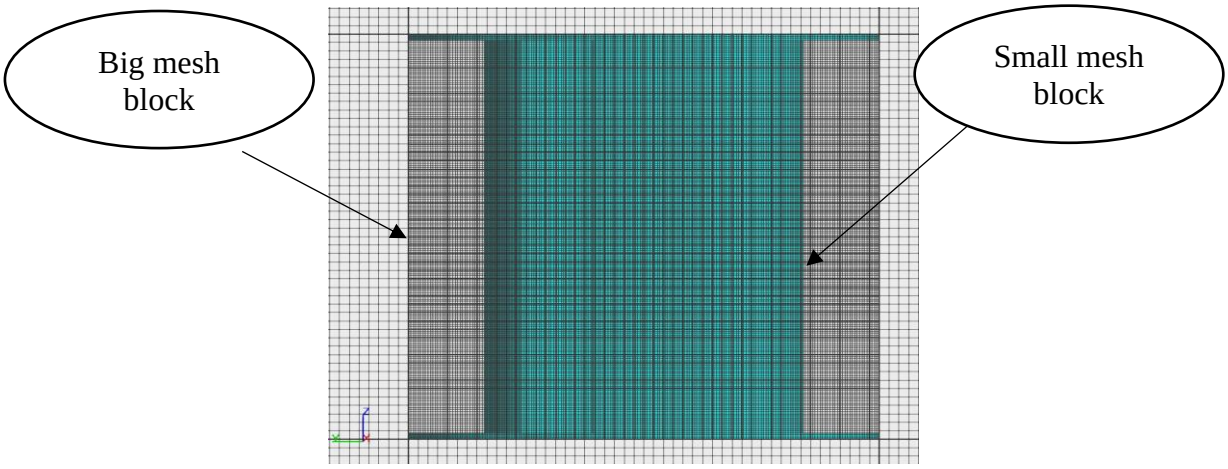

Figure 4.1: Mesh block size

4.2 CFD Results & Validation

As been mentioned in 3.7, CFD analysis must go through the validation process to assess their accuracy. In this work, the CFD results were compared with the data from the existing literature(Roy & Saha, 2015) to assess the accuracy before making modified model. For this purpose, CFD results of single stage Savonius turbine was compared with the experiment results as shown in Table 4.2.

Table 4.2 and Figure 4.2 is the experimental and CFD results of power coefficient while Table 4.3 and Figure 4.3 shows the experimental and CFD results for torque coefficient. From both Figure, the CFD value for all the TSR is higher than experimental results so the analysis is acceptable and can proceed to testing the modified hydrokinetic turbine. Table 4.2 also indicate that the maximum power coefficient is at TSR of 0.767 with the value of 0.279 for experimental and 0.298 for CFD.

Table 4.2: C_p values for experimental and CFD

TSR	**Experimental**	**CFD**	**Percentage of similarity (%)**
0.158	0.091	0.099	91.2
0.273	0.15	0.162	92.0
0.503	0.243	0.251	96.7
0.661	0.275	0.286	96
0.767	0.279	0.298	93.2
0.859	0.268	0.285	93.7
1.005	0.224	0.241	92.4
1.145	0.144	0.17	81.9

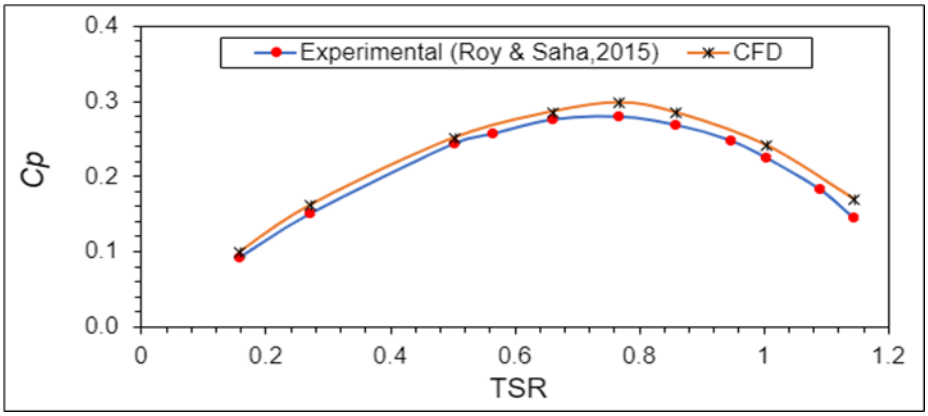

Figure 4.2: Graph of C_p experimental and CFD

Table 4.3: C_t experimental and CFD

TSR	Experimental	CFD	Percentage of similarity (%)
0.158	0.576	0.627	91.2
0.273	0.549	0.593	92
0.503	0.483	0.499	96.7
0.661	0.416	0.433	96
0.767	0.364	0.389	93.2
0.859	0.312	0.332	93.7
1.005	0.223	0.240	92.4
1.145	0.126	0.148	81.9

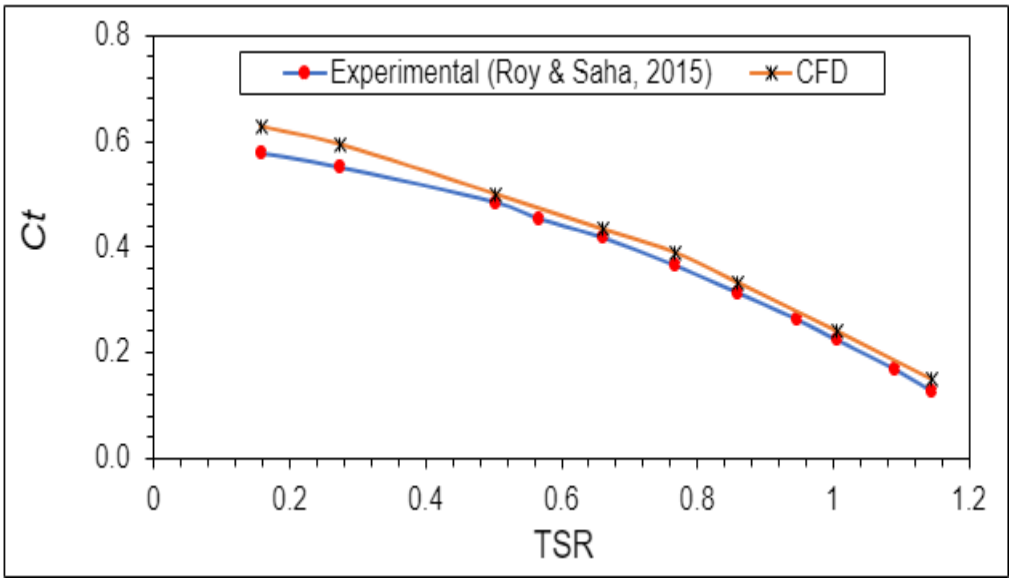

Figure 4.3: Graph of C_t experimental and CFD

4.3 C_p vs TSR

This section describes the power coefficient (C_p) results obtained for single stage and two stages at TSR intervals of 0.158-1.145 are shown in table 4.4 and graph figure 4.4. C_p in single stage continues to increase at TSR < 0.8 then decreases at TSR > 0.8. The C_{pmax} is 0.298 at TSR 0.767. Two stages also undergo the same pattern but the C_{pmax} is 0.322 higher than single stage at the same TSR, where C_{pmax} are same for both stages.

Table 4.4: TSR vs C_p for single and two stages

TSR	Single Stage	Two stages	Percentage of improvement (%)
0.158	0.099	0.087	-12.1
0.273	0.162	0.144	-11.1
0.503	0.251	0.269	7.2
0.661	0.286	0.311	8.7
0.767	0.298	0.322	8.1
0.859	0.285	0.303	6.3
1.005	0.241	0.251	4.1
1.145	0.17	0.192	12.9

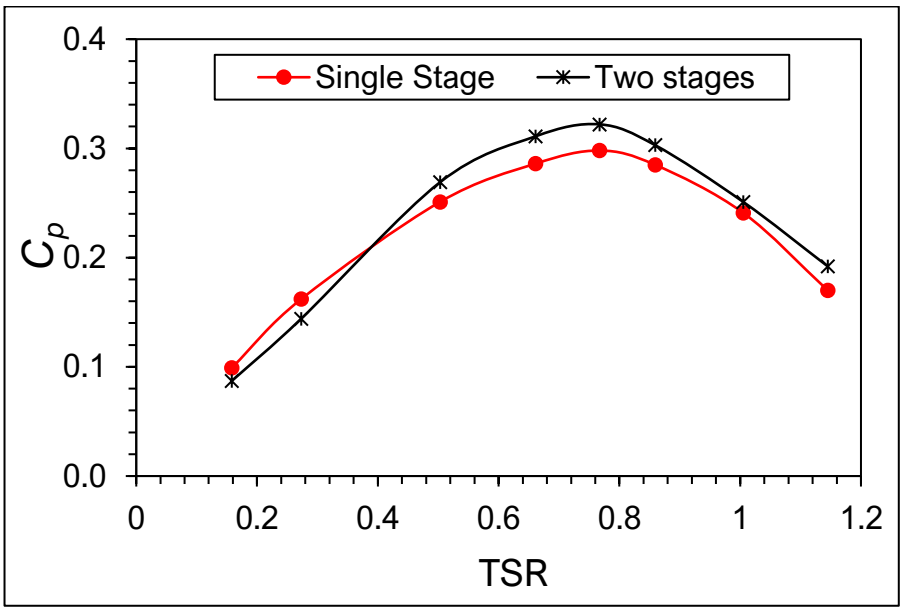

Figure 4.4: TSR vs C_p for single stage and two stages

4.4 C_t vs TSR

This section describes the torque coefficient (C_t) results obtained for single stage and two stages at TSR intervals of 0.158-1.145 are shown in Table 4.5 and graph figure 4.5. C_t in single stage gradually decreases from the starting TSR until 1.145. The C_{tmax} is 0.627 at TSR 0.158. C_t in two stage decreases then increased during 0.503 TSR whereases at TSR > 0.5 C_t value decreases. The C_{tmax} is 0.551 at TSR 0.627. The maximum value falls on the same TSR for both rotor.

Table 4.5: TSR vs C_t for single and two stages

TSR	Single Stage	Two Stages	Percentage of improvement (%)
0.158	0.627	0.551	-12.1
0.273	0.593	0.527	-11.1
0.503	0.499	0.535	7.2
0.661	0.433	0.470	8.7
0.767	0.389	0.420	8.1
0.859	0.332	0.353	6.3
1.005	0.240	0.250	4.1
1.145	0.148	0.168	12.9

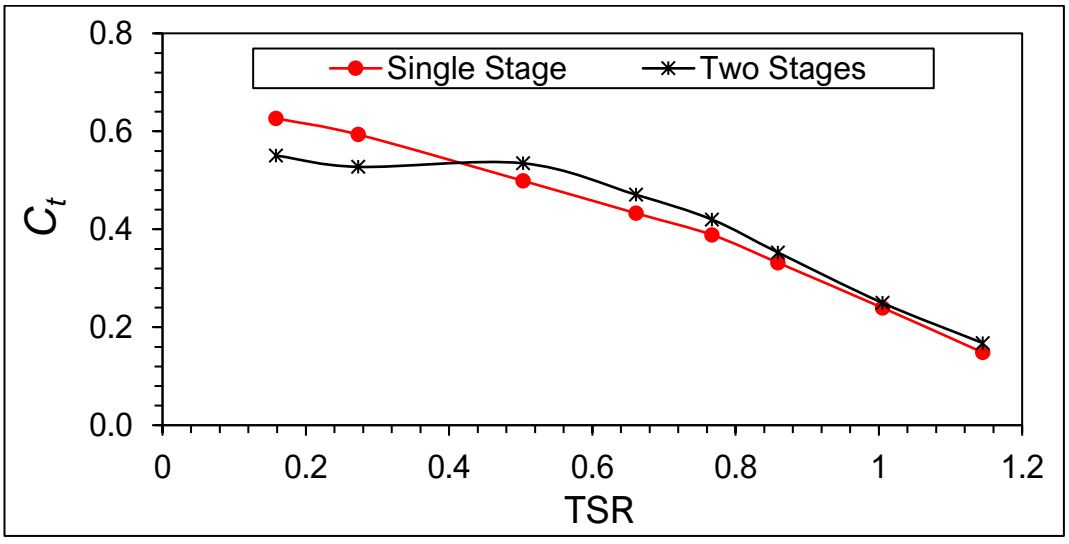

Figure 4.5: TSR vs C_t for single and two stages

Overall results, C_{pmax} and C_{tmax} for two stages is higher than single stage. For C_t the maximum value does not fall in the same TSR.

4.5 Torque Variations

Torque is an important factor in water turbine model. It is defined as moment or force that states certain objects rotates or stay static around the axis. It can measure the effectiveness of the force to produce rotation around the axis. Torque can be divided into two major categories, either static or dynamic. This category will be well-defined below. The torque is done for TSR 0.767 because the C_p is highest at this TSR.

4.5.1 Static Torque

Static Torque is the computations are performed without rotation of the rotor but at a different azimuthal angle. The variations of static torque versus the azimuthal angle are shown in Table 4.6 and Figure 4.6. From Figure 4.6, static torque has a different variation with varying the rotor angles for single and two stages. For a 0 angle, the two stages have a higher torque than the single stage. The blade achieved the maximum static torque because the flow strikes the concave side of advancing blades generate higher drag force, while the returning blades have a small drag force. The cycle repeated for one revolution. After 20-80 degree and 220-240 degree, the static torque decreased which minimum static torque occurred at 180 degrees. For the 0-180 degree, the maximum static achieved by single stage is at 20^0 with the value of 0.397 while for two stages the value is at 0.459 at 80 degree. The static torque appears similar after 180 degrees. At the angle of 240^0 the static torque coefficient is high positive values for two stages and for single stage the high positive value is at 220 degree.

Table 4.6: Static torque for single stage and two stages

Azimuthal angle	Single Stage	Two Stages
0	0.092	0.118
20	0.397	0.342
80	0.371	0.459
100	0.228	0.317
120	0.136	0.253
180	0.092	0.118
200	0.4	0.342
220	0.482	0.464
240	0.468	0.548
260	0.365	0.459
280	0.234	0.317
300	0.134	0.253
320	0.087	0.18
340	0.05	0.146
360	0.092	0.118

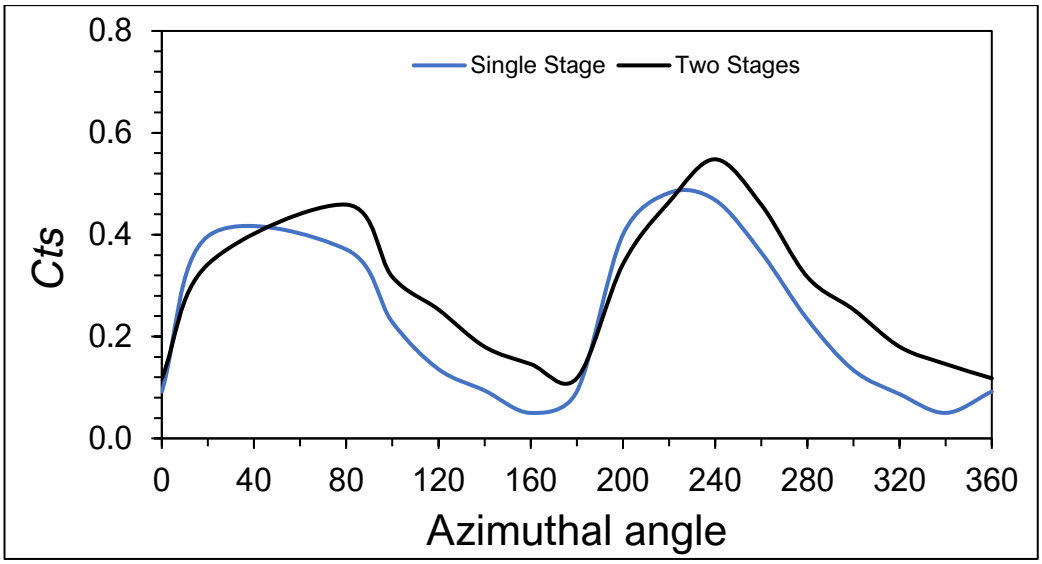

Figure 4.6: Static torque for single stage and two stages

4.5.2 Dynamic Torque

Dynamic force involve acceleration where static force does not. It rotates at its own axis but at a different azimuthal angle. Figure 4.7 shows the dynamic torque coefficients variation in one revolution at TSR of 0.767. There is negative value torque for single stage at 160 and 340 degrees. This is because the blade is in returning position. Single stage and two stages have the same maximum torque which is 0.59 and 0.659 respectively. Single stage obtained the highest torque at 80 and 260 degree while the two stages obtained at 100 and 280 degree. The two stages generate higher power since it eliminates the negative torque.

Table 4.7: Dynamic torque for single stage and two stages

Azimuthal angle	Single Stage	Two Stages
0	0.231	0.262
20	0.391	0.431
80	0.59	0.631
100	0.528	0.659
160	-0.068	0.029
180	0.231	0.262
200	0.391	0.431
220	0.461	0.52
240	0.533	0.576
260	0.59	0.631
280	0.528	0.659
300	0.393	0.458
320	0.198	0.223
340	-0.068	0.029
360	0.231	0.262

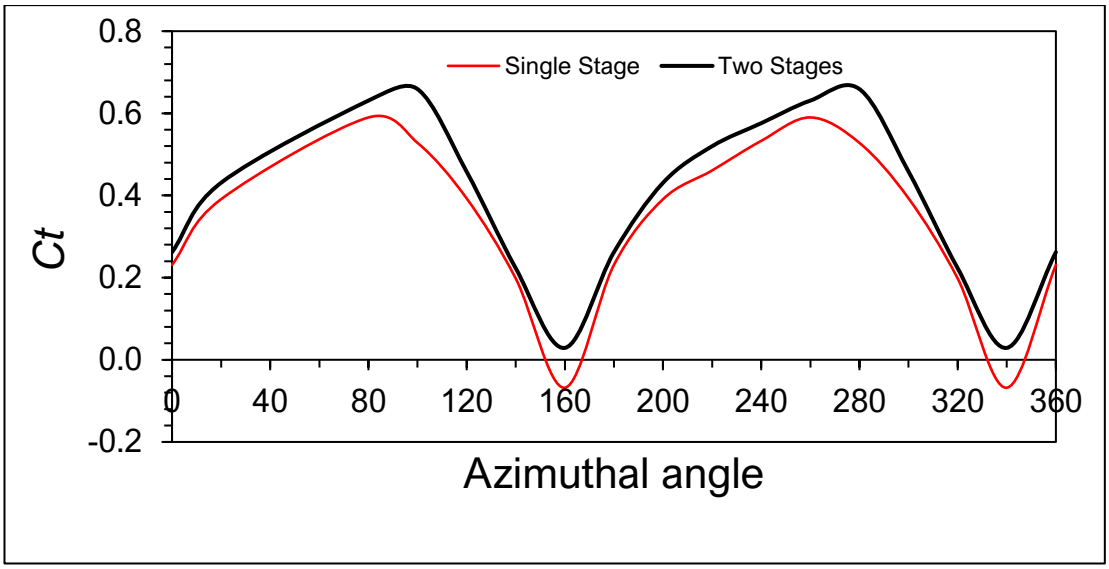

Figure 4.7: Dynamic torque for single stage and two stages

4.6 Drag Coefficient

Regarding to Figure 4.8, it can be observed that the minimum drag coefficients of all single stage are produced in the phase angle of 90 degrees whereas the maximum is produced in the phase angle of about 180°. While for the two stage, the minimum drag coefficients are in the phase angle of 120 and maximum produced at the 0 angle. It is also remarkable that all the values are positive at any phase angle. The minimum value of drag coefficient is about 0.27 and 0.41 for single stage and two stages respectively. Then, the maximum value is 0.98 and 1.13 for both stages.

Table 4.8: Drag coefficient for single stage and two stages

Angle	Single Stage	Two Stages
0	0.94	1.13
30	0.74	0.93
60	0.63	0.76
90	0.27	0.66
120	0.43	0.41
150	0.72	0.84
180	0.98	1.04
210	0.83	0.79
240	0.59	0.64
270	0.38	0.51
300	0.52	0.75
330	0.79	0.94
360	0.92	1.07

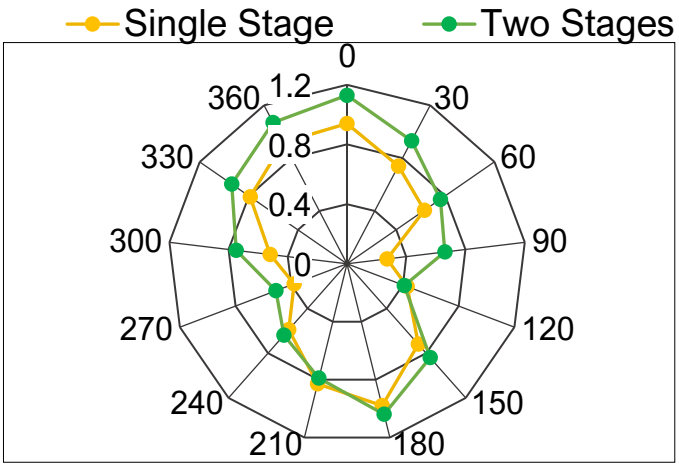

Figure 4.8: Drag coefficient for single stage and two stages

4.7 Discussion on turbulence intensity and velocity

4.7.1 Downstream turbulence intensity

From the Table and Figure below, two stages have a higher turbulence intensity then the single stage. The turbulence intensity was generated for TSR 0.767. Approximately after 4D downstream, the turbulence intensity decreases for both stages. The optimum downstream for distance is 4D since the turbulence intensity is high.

Table 4.9: Turbulence intensity for single stage and two stages

Downstream distance	Single Stage	Two Stages
2D	22.3	25.1
4D	27.6	31.7
5.5D	25.4	28.2

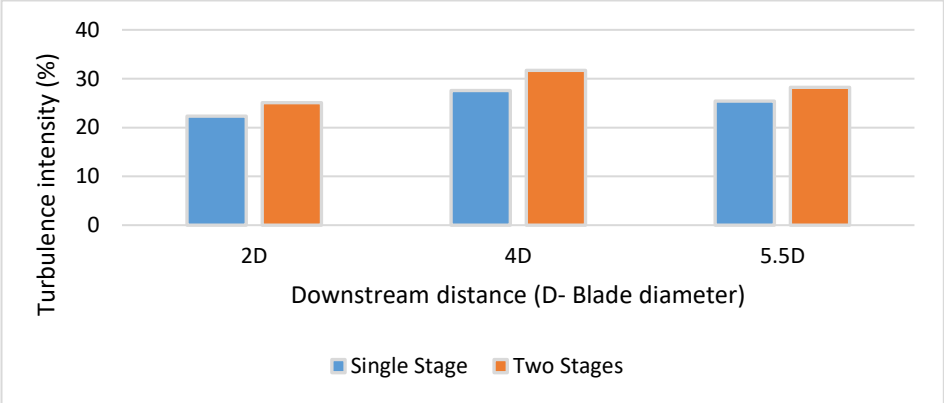

Figure 4.9: Turbulence intensity difference for single stage and two stages

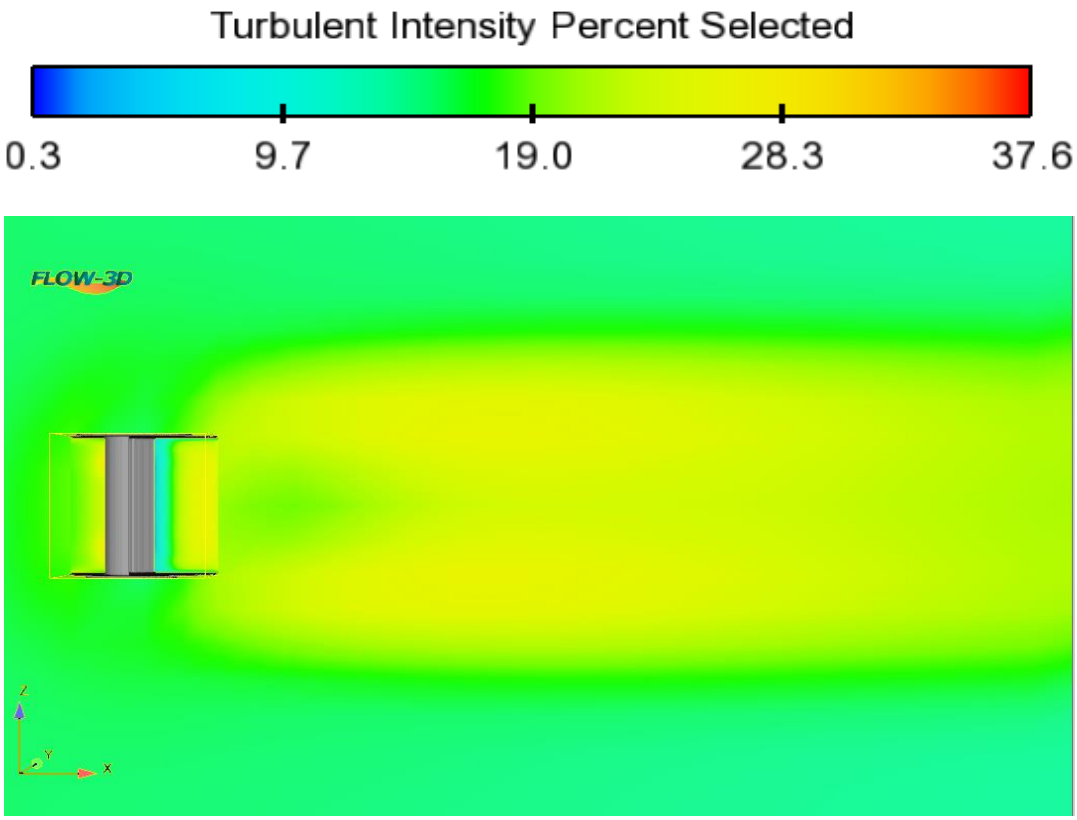

Figure 4.10: Turbulence intensity flow for single stage

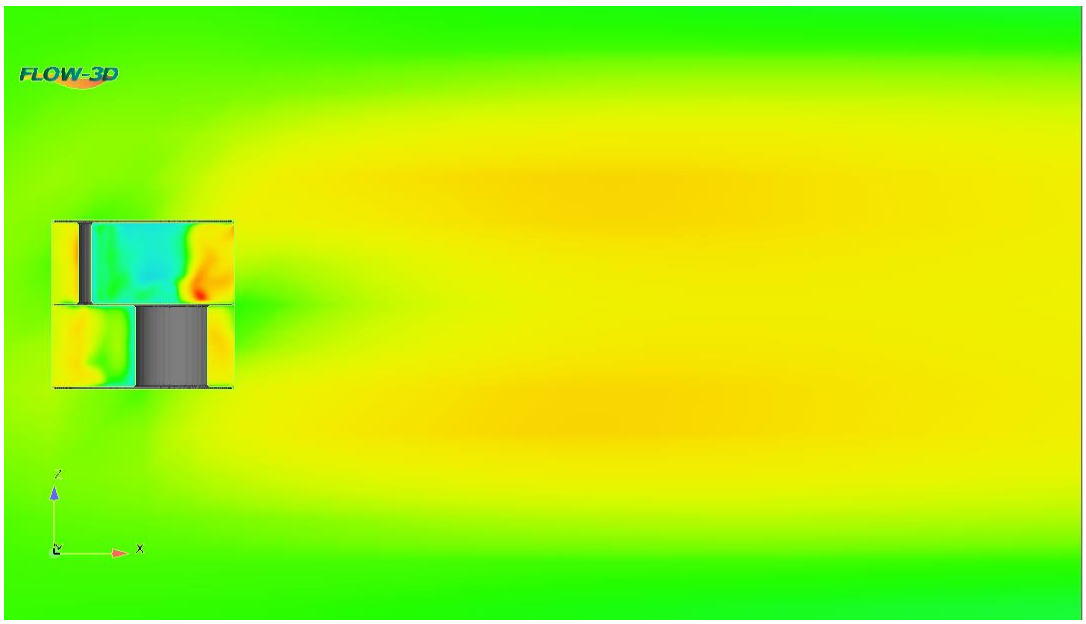

Figure 4.11: Turbulence intensity flow for two stages

4.7.2 Downstream Flow Velocity

Power output is depending on the velocity flow. As can be seen in the figure, the velocity flow is less since the water losses the energy behind the turbine. After the water flows through the turbine, it regains back the kinetic energy, so the velocity increases gradually. Single stage has a higher velocity flow at 1D than two stages because kinetic energy regaining in a shorter distance. Then two stages recorded higher velocity flow then single stage. The flow velocity is generated for TSR 0.767.

Table 4.10: Flow Velocity for single stage and two stages

Downstream distance	Single Stage	Two Stages
1D	0.28	0.21
2.5D	0.33	0.37
4D	0.42	0.44
5.5D	0.51	0.58

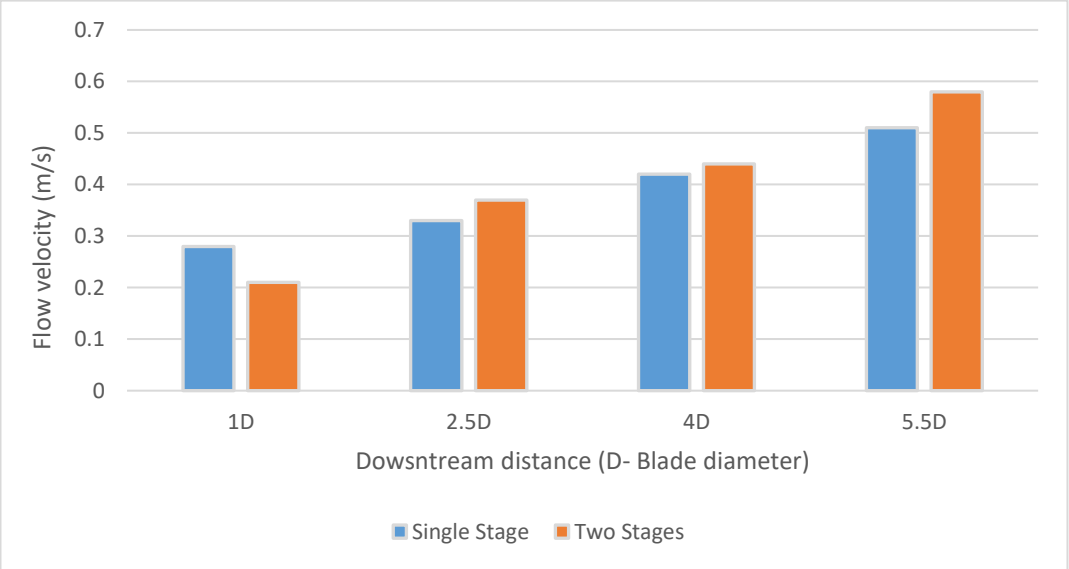

Figure 4.12: Flow Velocity for single stage and two stages

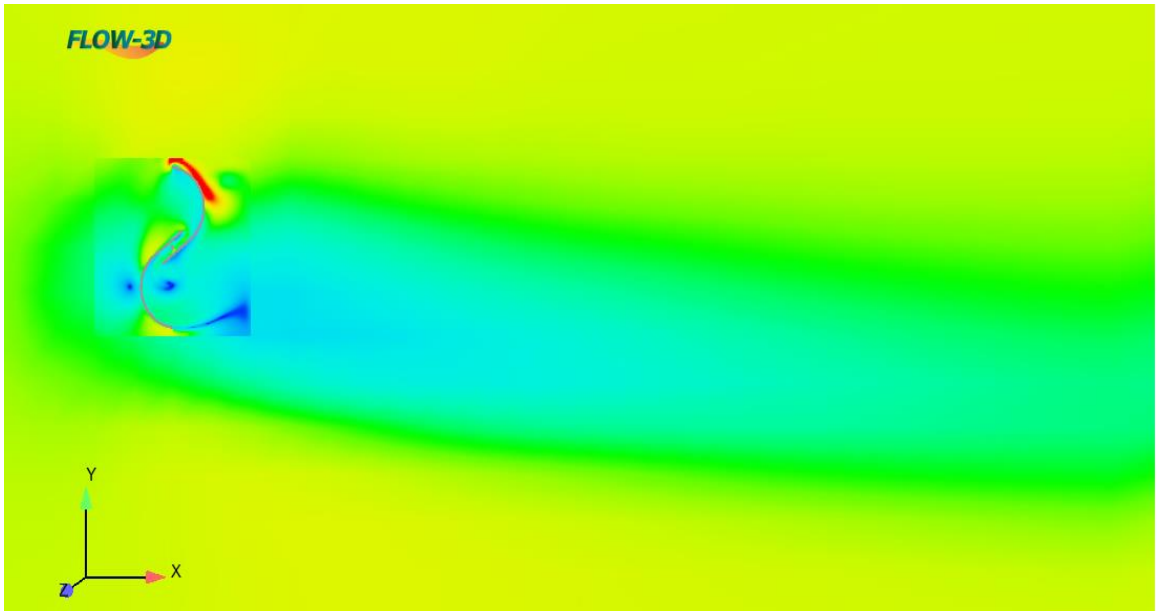

Figure 4.13: Flow Velocity for single stage

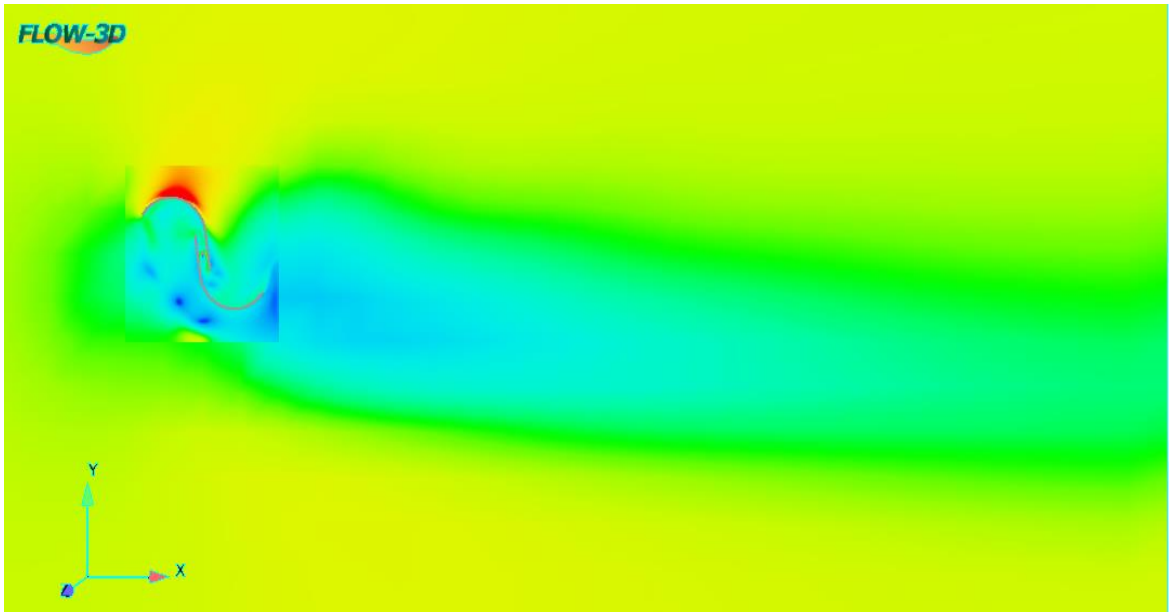

Figure 4.14: Flow Velocity for two stages

4.8 Pressure contour

Figure 4.15 and 4.16 shows the pressure contour for single stage and two stages turbine. Concave surface (inner curve blade) has a higher pressure than the convex surface (outer curve blade). This pressure causes the blade to rotate in clockwise direction.

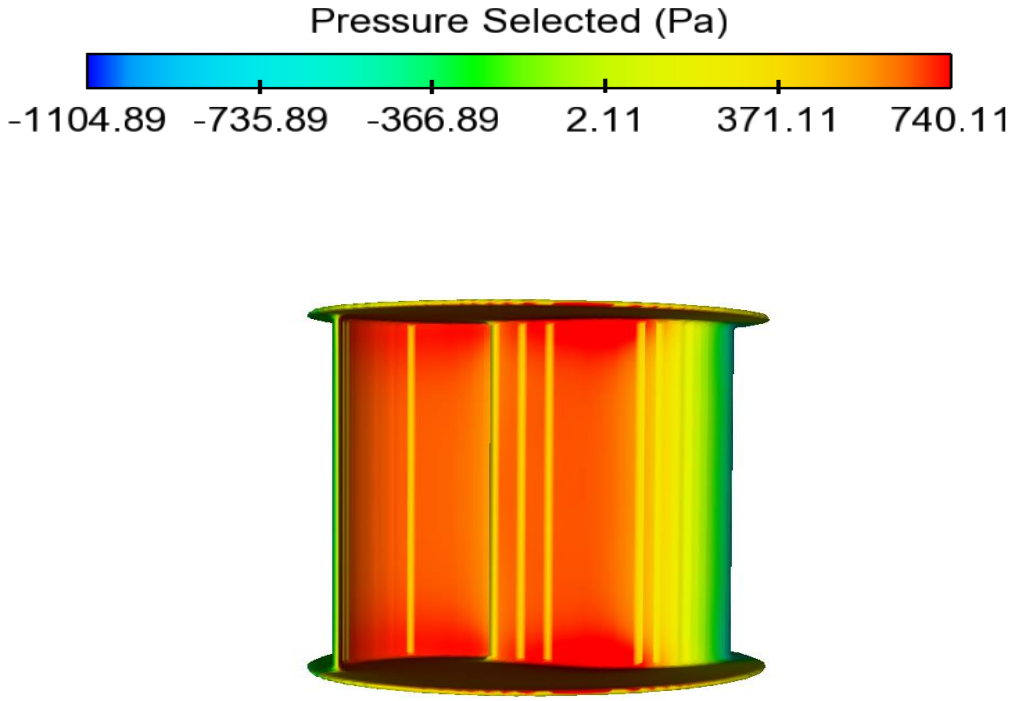

Figure 4.15: Pressure contour for single stage

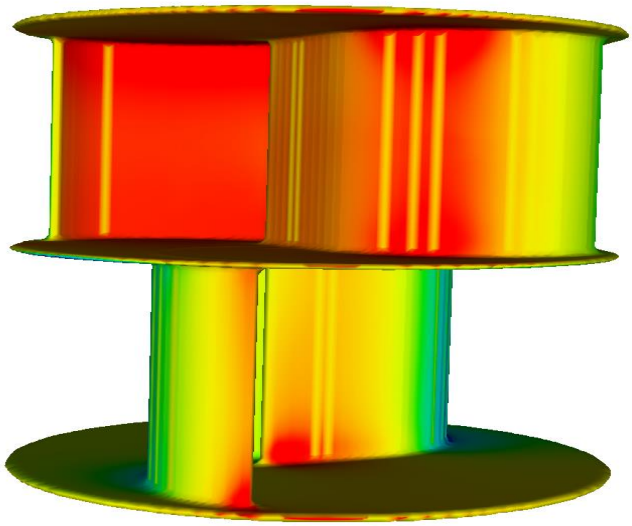

Figure 4.16: Pressure contour for two stages

4.9 Comparison of Economical Aspects

Table 4.11: Economical aspects for single stage and two stages

Parameters	**Single Stage Bach**	**Two stages Bach**
Turbine efficiency, η_T	30%	32.2%
Generator efficiency, η_G	80%	80%
Transmission-storage efficiency, η_{TS}	70%	70%
Overall efficiency of turbine, η_O	16.8%	18.0%
Available power in the wind, W	264.2	264.2
Power output	44.4W	47.6 W
Power output in kWh per day	1.07	1.14
Power cost per kWh	0.35USD	0.35USD
Turbine capital cost	400 USD	400 USD
Maintenance cost	100 USD	100 USD
Payback Period, years	3.7	3.4

The overall efficiency and the power output of single stage and two stages are calculated using the following equation:

$$\eta_O = \eta_T \; x \; \eta_G \; x \; \eta_{TS}$$

η_T, η_G and η_{TS} are the efficiency corresponds to the wind turbine, electric generator and transmissions and storage system respectively.

Power output of both stages = Power available in the wind x overall efficiency

$$= 1/2 \; pAV^3 \; x \; \eta_O$$

Cpmax of the two stages is 32.2%, η_G = 80% (commonly found efficiency) and η_{TS} = 70% (considering a maximum loss), the overall efficiency of the two stages is estimated to be 18%. The overall efficiency for modified Bach is estimated to be 16.8%. To calculate the payback period, it is assumed that the capital cost and maintenance cost to be 400 USD and 100 USD, the payback period for involving the double stage is calculated by the following equation(Roy & Saha, 2015):

Payback Period= $\frac{Total\ Cost}{Power\ cost\ per\ kWh\ x\ Power\ output\ in\ kWh}$

$= \frac{400+100}{1.14\ x\ 0.35}$

=1253.13 days

=3.4 years

Table 4.9.1 shows the details of the economical aspects regarding on the payback period for all the turbine types using the equations. It has been observed that the payback period for two stages is lesser than the single stage since it has a higher efficiency.

CHAPTER 5

CONCLUSION & RECOMMENDATION

5.1 Conclusion

The study aimed at achieving an optimized design of hydrokinetic turbine suitable for low-velocity river applications. For this study, the modified Bach Savonius turbine was selected as the base model owing to its better performance reported in the literature as compared to the conventional Savonius. The modified Bach turbine was initially modeled and validated with the existing experimental results using 3D CFD simulations. Later, the optimization technique of multi-staging was employed, and a two stages Bach design was designed. The performance evaluation of the modified two stages Bach design was conducted at the similar Reynold's number of $6.0\,x\,10^4$. From the comparison of obtained results, it was found that the torque extraction capacity of modified two stages Bach model was improved by 12.9%. The better torque extraction subsequently enhanced the C_p value by 8.1%. Also, it was observed that the two stages turbine showed lower torque fluctuations which implies that the optimized turbine will suffer from less vibration forces. Taking into consideration the low-flow velocity of 0.86 m/s used for the simulations, the reported efficiency of 32.2% can be considered as notably upgraded. Furthermore, comparisons were drawn on the economical aspects for both the single stage Bach and the two-staged Bach. Owing to the improved efficiency for the two stages turbine a lower payback period of 3.4 years for the investments was calculated as compared to the 3.7 year period for the single-stage turbine. The main objective of this dissertation is to increase the performance of existing hydrokinetic turbine for low-speed river current by modifying the existing hydrokinetic turbine.

5.2 Recommendation and Future Work

Current work has discovered some improvement to the rotor. The following are further works that can be done to obtain a better result for the Savonius hydrokinetic turbine such as:

a) An experimental or simulation on more than two stages Savonius hydrokinetic turbine. Since the two stage SHT generate better performances than single stage. Increases in stages may improve the overall performance of the turbine. Thus, the study can be done on testing three stage, four stages and five stages and analyze the power coefficient.

b) A study on the effects of different position of the deflector in two stage Savonius hydrokinetic turbine. In this current work, deflector was not used. Since there are studies stating that using deflector in the turbine improves the rotor performance. Hence, a study can be done on the position of deflector at the returning blade side.

c) The study can be continued to investigate the effect of different blade's shape on performance of turbine. The blades play an important role in the turbine operation, because it is exposed to the water and rotates. The types of blade's shapes may have significant effect on the turbine performance.

REFERENCES

Agency, I. E. (April 2020). *Global Energy Review*. Retrieved from https://www.iea.org/reports/global-energy-review-2020

Association, I. H. (May 3, 2016). Global installed hydropower capacity by country at the end of 2015. Retrieved from http://www.nepalenergyforum.com/global-installed-hydropower-capacity-by-country-at-the-end-of-2015/

Alexander N. Gorban', A. M. G., Valentin M. Silantyev. (December 2001). Limits of the Turbine Efficiency for Free Fluid Flow. *Journal of Energy Resources Technology, Vol. 123*. doi:DOI: 10.1115/1.1414137

Alizadeh, H., Jahangir, M. H., & Ghasempour, R. (2020). CFD-based improvement of Savonius type hydrokinetic turbine using optimized barrier at the low-speed flows. *Ocean Engineering, 202*. doi:10.1016/j.oceaneng.2020.107178

Alom, N., & Saha, U. K. (2019). Evolution and Progress in the Development of Savonius Wind Turbine Rotor Blade Profiles and Shapes. *Journal of Solar Energy Engineering, 141*(3). doi:10.1115/1.4041848

Association, I. H. (May 3, 2016). Global installed hydropower capacity by country at the end of 2015. Retrieved from http://www.nepalenergyforum.com/global-installed-hydropower-capacity-by-country-at-the-end-of-2015/

Badrul Salleh, M., Kamaruddin, N. M., & Mohamed-Kassim, Z. (2019). Savonius hydrokinetic turbines for a sustainable river-based energy extraction: A review of the technology and potential applications in Malaysia. *Sustainable Energy Technologies and Assessments, 36*. doi:10.1016/j.seta.2019.100554

Basumatary, M., Biswas, A., & Misra, R. D. (2018). CFD analysis of an innovative combined lift and drag (CLD) based modified Savonius water turbine. *Energy Conversion and Management, 174*, 72-87. doi:10.1016/j.enconman.2018.08.025

Behrouzi, F., Nakisa, M., Maimun, A., & Ahmed, Y. M. (2016). Global renewable energy and its potential in Malaysia: A review of Hydrokinetic turbine

technology. *Renewable and Sustainable Energy Reviews, 62*, 1270-1281. doi:10.1016/j.rser.2016.05.020

BP. (1996-2020). Statistical Review of World Energy. Retrieved from https://www.bp.com/en/global/corporate/energy-economics/statistical-review-of-world-energy.html

C. Boccaletti, G. F., J.Marco, E. Santini. An Overview on Renewable Energy Technologies for Developing Countries: the case of Guinea Bissau.

Council, W. E. (2016). *World-Energy-Resources*. Retrieved from https://www.worldenergy.org/assets/images/imported/2016/10/World-Energy-Resources-Full-report-2016.10.03.pdf

Evans, A., Strezov, V., & Evans, T. J. (2009). Assessment of sustainability indicators for renewable energy technologies. *Renewable and Sustainable Energy Reviews, 13*(5), 1082-1088. doi:10.1016/j.rser.2008.03.008

Golecha, K., Eldho, T. I., & Prabhu, S. V. (2011). Influence of the deflector plate on the performance of modified Savonius water turbine. *Applied Energy, 88*(9), 3207-3217. doi:10.1016/j.apenergy.2011.03.025

Golecha Kailash, T. I. E., and S. V. Prabhu. (2012). Performance Study of Modified Savonius Water Turbine with Two Deflector Plates. *International Journal of Rotating Machinery, 2012*, 1-12. doi:10.1155/2012/679247

Headquarters, N. G. (1996 - 2020). Retrieved from https://www.nationalgeographic.org/encyclopedia/non-renewable-energy/

International Energy Outlook (October 14, 2020). Retrieved from https://www.eia.gov/outlooks/ieo/

Jing, F., Sheng, Q., & Zhang, L. (2014). Experimental research on tidal current vertical axis turbine with variable-pitch blades. *Ocean Engineering, 88*, 228-241. doi:10.1016/j.oceaneng.2014.06.023

Jones, N. F., Pejchar, L., & Kiesecker, J. M. (2015). The Energy Footprint: How Oil, Natural Gas, and Wind Energy Affect Land for Biodiversity and the Flow of Ecosystem Services. *BioScience, 65*(3), 290-301. doi:10.1093/biosci/biu224

Kacprzak, K., & Sobczak, K. (2014). Numerical analysis of the flow around the Bach-type Savonius wind turbine. *Journal of Physics: Conference Series, 530*. doi:10.1088/1742-6596/530/1/012063

Kailash, G., Eldho, T. I., & Prabhu, S. V. (2012). Performance Study of Modified Savonius Water Turbine with Two Deflector Plates. *International Journal of Rotating Machinery, 2012*, 1-12. doi:10.1155/2012/679247

Kumar, A., & Saini, R. P. (2016). Performance parameters of Savonius type hydrokinetic turbine – A Review. *Renewable and Sustainable Energy Reviews, 64*, 289-310. doi:10.1016/j.rser.2016.06.005

Laniyi Ladokun, A. K. R., B. F. Sule. (November 2013). Hydrokinetic energy conversion systems: Prospects and challenges in Nigerian hydrological setting.

Laws, N. D., & Epps, B. P. (2016). Hydrokinetic energy conversion: Technology, research, and outlook. *Renewable and Sustainable Energy Reviews, 57*, 1245-1259. doi:10.1016/j.rser.2015.12.189

Liu, F., Tait, S., Schellart, A., Mayfield, M., & Boxall, J. (2020). Reducing carbon emissions by integrating urban water systems and renewable energy sources at a community scale. *Renewable and Sustainable Energy Reviews, 123*. doi:10.1016/j.rser.2020.109767

Mahalingam Venkatesh, P., Vijay Babu, A. R., & Suresh, K. (2018). Experimental investigations on modified Savonius wind turbine with curtain arrangements in the middle of the highway. *European Journal of Electrical Engineering, 20*(3), 267-278. doi:10.3166/ejee.20.267-278

Mahesa Prabowoputra, D., Hadi, S., Sohn, J. M., & Prabowo, A. R. (2020). The effect of multi-stage modification on the performance of Savonius water turbines under the horizontal axis condition. *Open Engineering, 10*(1), 793-803. doi:10.1515/eng-2020-0085

Mohamed, M. H., Janiga, G., Pap, E., & Thévenin, D. (2010). Optimization of Savonius turbines using an obstacle shielding the returning blade. *Renewable Energy, 35*(11), 2618-2626. doi:10.1016/j.renene.2010.04.007

Mosbahi, M., Lajnef, M., Derbel, M., Mosbahi, B., Aricò, C., Sinagra, M., & Driss, Z. (2021). Performance Improvement of a Drag Hydrokinetic Turbine. *Water, 13*(3). doi:10.3390/w13030273

Nahidul Islam Khan, T. I., Michael Hinchey,Vlastimil Masek. (2009). Describe the performance of three different types of Savonius rotor as current-driven turbines for micro-power generation. *Journal of Ocean Technology 2009,Maritime and Port Security, Vol. 4, No. 2*.

Nahidul Khan, V. M., Tariq Iqbal. (2009). Performance of Savonius rotor as a water current turbine.

Nakajima, M., Iio, S., & Ikeda, T. (2008). Performance of Double-step Savonius Rotor for Environmentally Friendly Hydraulic Turbine. *Journal of Fluid Science and Technology, 3*(3), 410-419. doi:10.1299/jfst.3.410

Omar Yaakob, M. A. I., Yasser M. Ahmed. (2012). Validation Study for Savonius Vertical Axis Marine Current Turbine Using CFD Simulation.

Omar bin Yaakob, K. K. K. (2013). The Promise of Marine Renewable Energy in Malaysia: Too Good To Be True? . *Malaysian Journal of Science 32*(SCS Sp Issue), 309-316.

Parag K. Talukdara, A. S., Vinayak Kulkarnia, Ujjwal K. Sahaa. (2008).

Ragheb, M. R. a. A. M. (2011). Wind Turbines Theory - The Betz Equation and Optimal Rotor Tip Speed Ratio. *Fundamental and Advanced Topics in Wind Power*.

Renewable energy consumption, World. Retrieved from https://ourworldindata.org/grapher/renewable-energy-consumption?country=~OWID_WRL

Roy, S., & Saha, U. K. (2015). Wind tunnel experiments of a newly developed two-bladed Savonius-style wind turbine. *Applied Energy, 137*, 117-125. doi:10.1016/j.apenergy.2014.10.022

Sarma, N. K., Biswas, A., & Misra, R. D. (2014). Experimental and computational evaluation of Savonius hydrokinetic turbine for low velocity condition with comparison to Savonius wind turbine at the same input power. *Energy Conversion and Management, 83*, 88-98. doi:10.1016/j.enconman.2014.03.070

Sarma, N. K. (2014). *Experimental and CFD analyses of two bladed savonius water turbine under low velocity conditions.* Paper presented at the ASME 2014 Power Conference, Baltimore, Maryland, USA.

Tian, W., Mao, Z., & Ding, H. (2018). Design, test and numerical simulation of a low-speed horizontal axis hydrokinetic turbine. *International Journal of Naval Architecture and Ocean Engineering, 10*(6), 782-793. doi:10.1016/j.ijnaoe.2017.10.006

Tian, Y., Zhang, F., Yuan, Z., Che, Z., & Zafetti, N. (2020). Assessment power generation potential of small hydropower plants using GIS software. *Energy Reports, 6*, 1393-1404. doi:10.1016/j.egyr.2020.05.023

Tony Burton, D. S., Nick Jennis, Ervin Bossanyi. (2001). *Wind_Energy_Handbook.pdf*.

Ulvmyr, A. (June 2016). *Potential risks and prospects of protections of a hydrokinetic turbine implemented in the Amazon River, Colombia.* Karlstad University, 651 88 Karlstad.

V.J.Modi, M. S. U. K. F. a. N. J. R. Aerodynamics of the savonius rotors : Experiments and analysis.

Wikipedia. Renewable Energy. Retrieved from https://en.wikipedia.org/wiki/Renewable_energy

Wikipedia. (15 November 2020). Hydroelectricity. Retrieved from https://en.wikipedia.org/wiki/Hydroelectricity

Wise, E. (2020). Retrieved from https://www.edfenergy.com/for-home/energywise/renewable-energy-sources

Zhou, Z., Benbouzid, M., Charpentier, J.-F., Scuiller, F., & Tang, T. (2017). Developments in large marine current turbine technologies – A review. *Renewable and Sustainable Energy Reviews, 71*, 852-858. doi:10.1016/j.rser.2016.12.113